'On the Role of Beamforming in Technical Acoustics', or: Purpose and parameters of phased arrays (microphone antennas)

M. Möser

November 10, 2006

Contents

Part 1

Purposes and applications of phased arrays

1.1 Source location and identification

Example 1: Factory

Fig. 1.1: Some 'noisy' environment in front of a plant (courtesy from GFaI)

Example 2: Motorcompartment

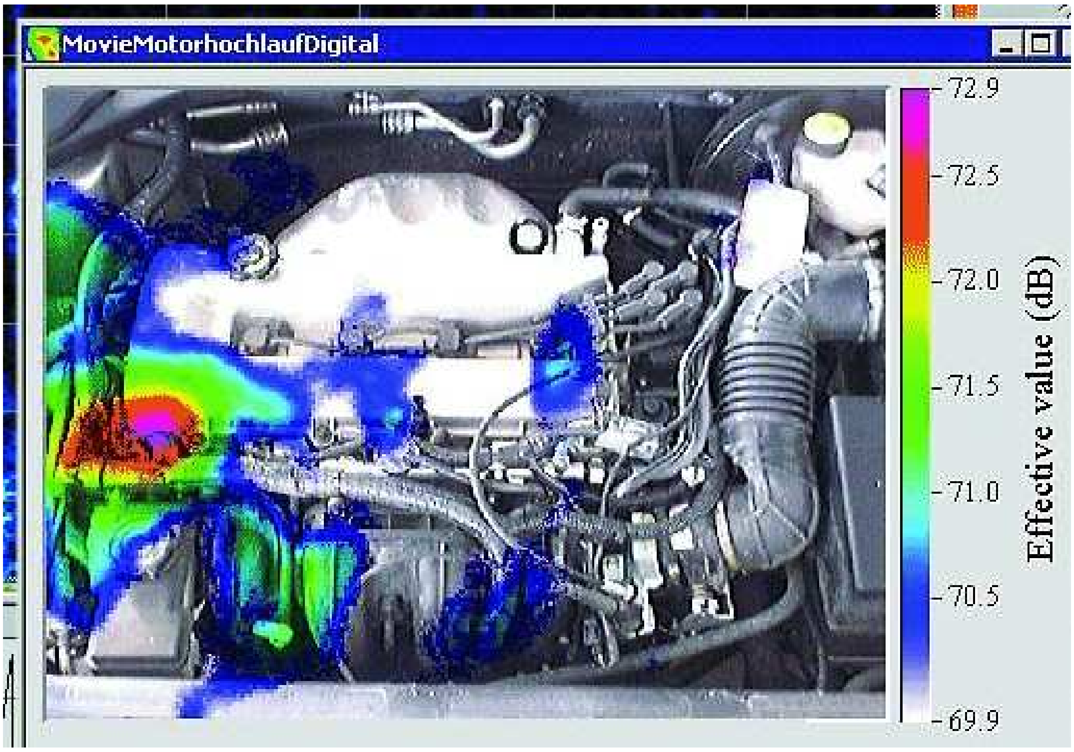

Fig. 1.2: Sources inside a motorcompartment (courtesy from GFaI)

Example 3: Train passby

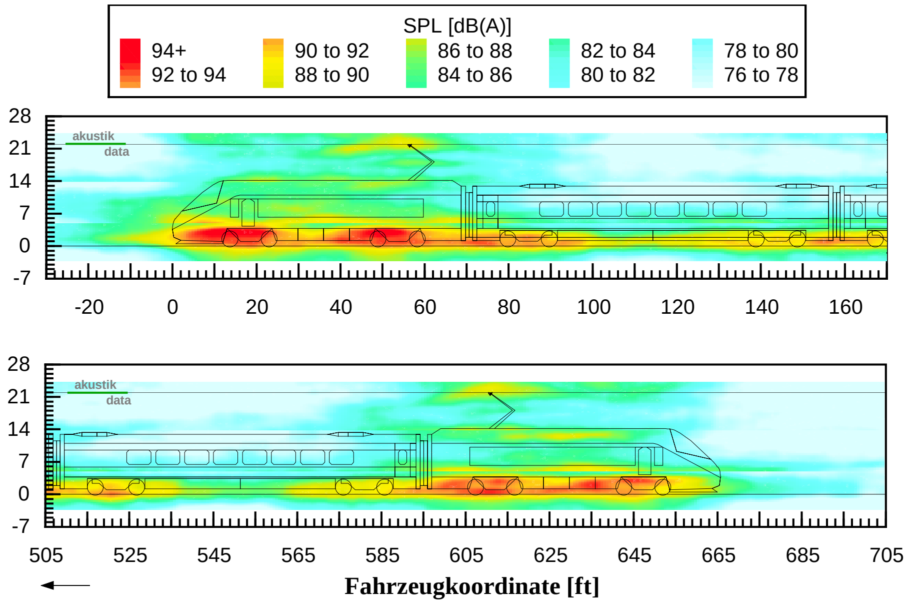

Fig. 1.3: Sound sources from a train passby (courtesy from Akustik-Data)

Example 4: Van

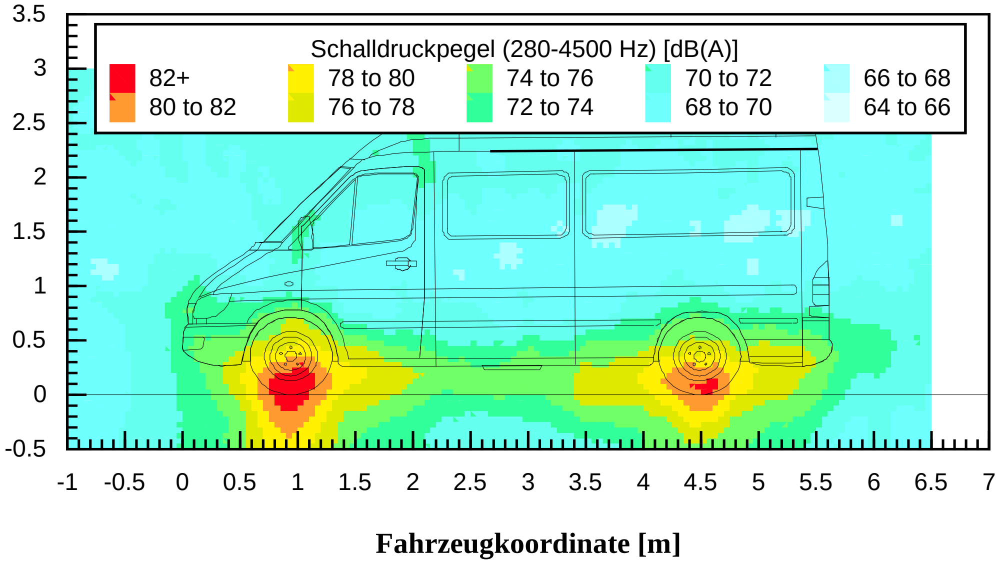

Fig. 1.4: Sound sources from a van passby (courtesy from Akustik-Data))

1.2 Improvement of signal to noise ratio

Typical situation for measurements in cities

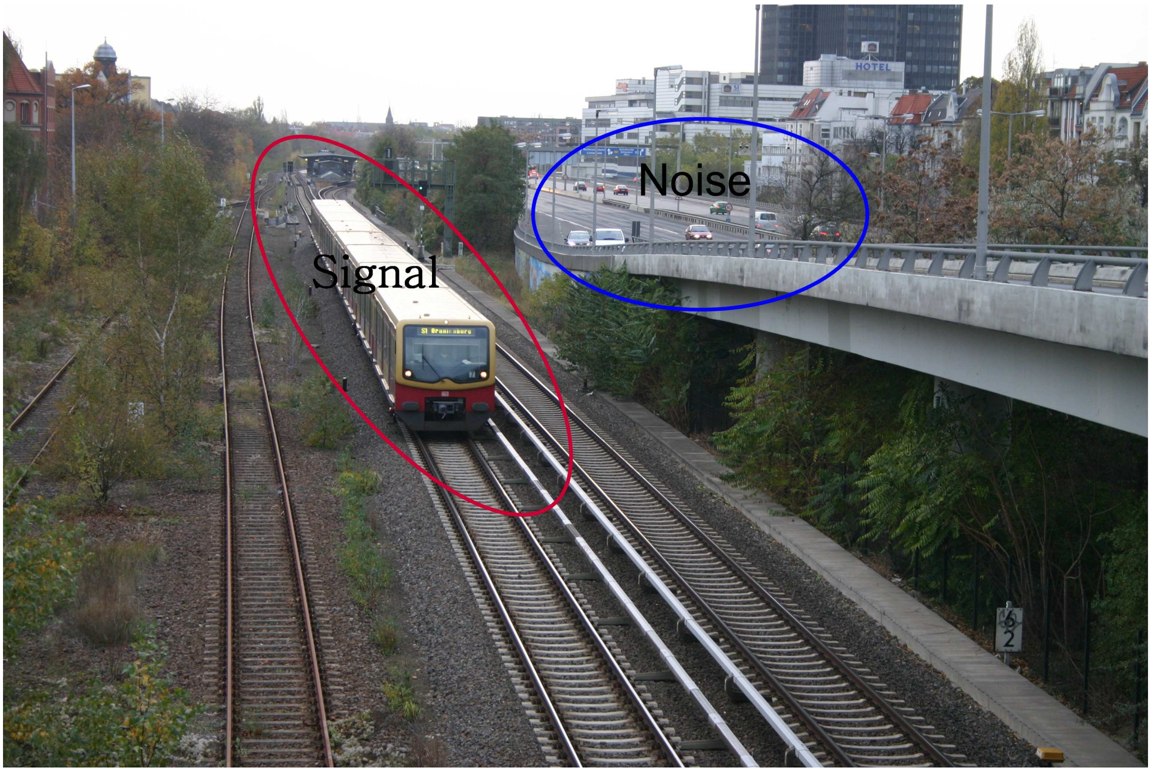

Fig. 1.5: Measurement of the sound from a train passby next to a street

Fig. 1.6: Soundreducing headpiece (SSI: Sound Screen Improver) on a wall (near Innsbruck)

Fig. 1.7: Layout of SSI (from 'top')

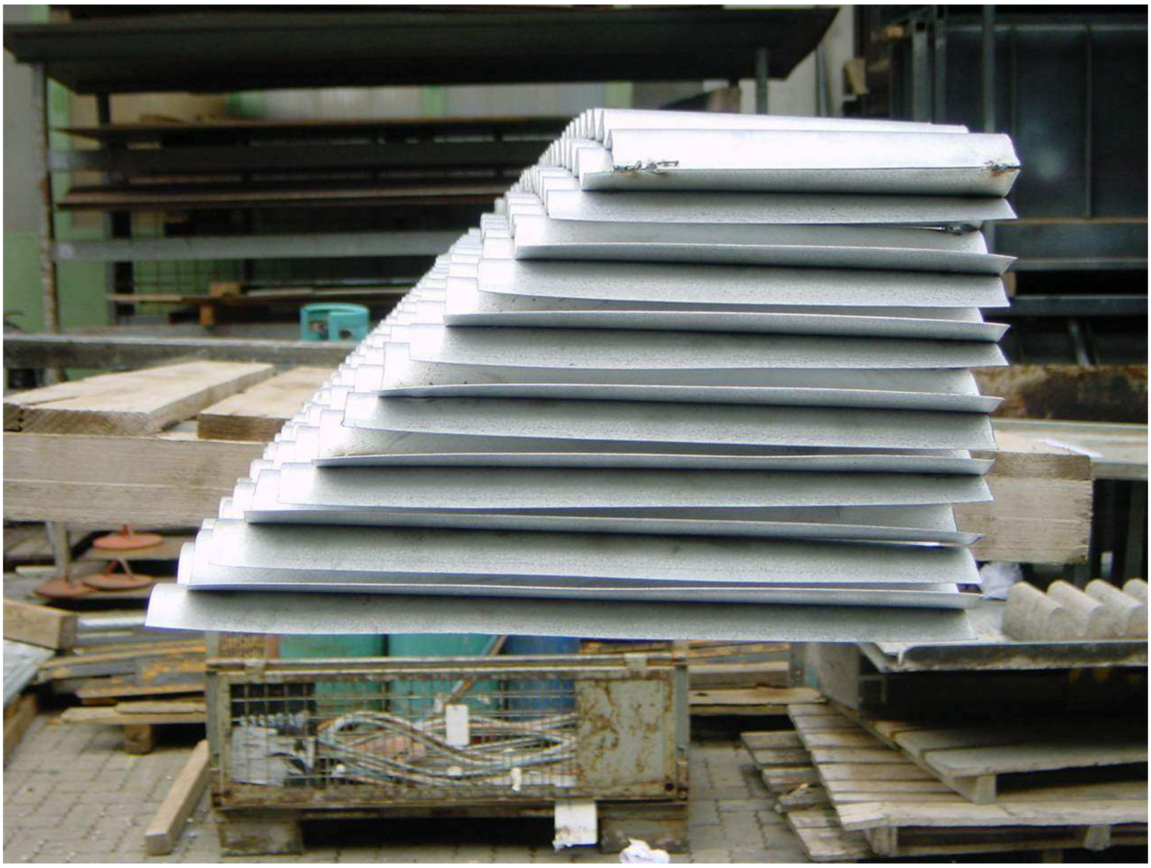

Fig. 1.8: Layout of SSI (from 'side')

Fig. 1.9: Layout of SSI (from below when mounted)

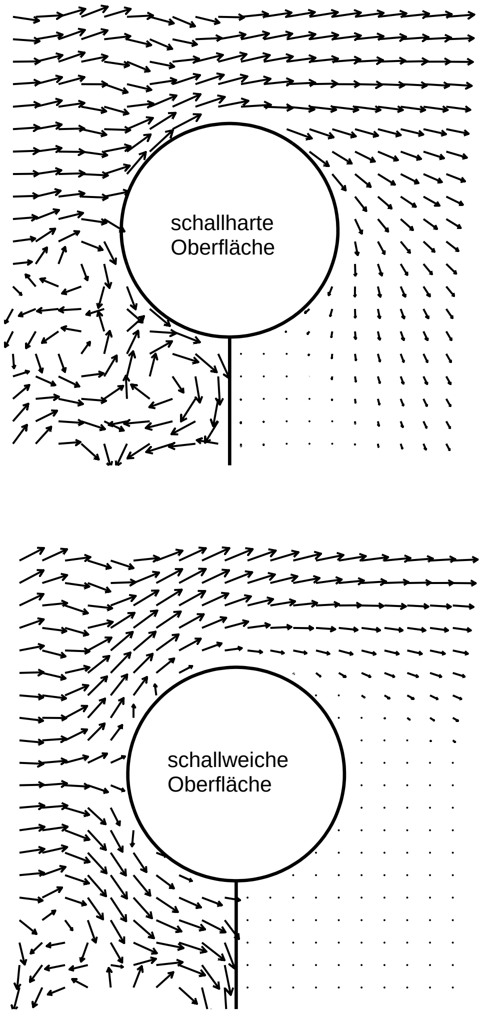

Fig. 1.10: Intensity flow (in dB) near a rigid (above) and an ideal elastic (zero-pressure, below) headpiece

Calculation of MEASURED improvement $\Delta L(meas)$ for true improvement ΔL and signal-to-noise-ratio S:

$$\Delta L = 10\,\lg\left(1 + 10^{-S/10}\right) - 10\,\lg\left(10^{-\Delta L/10} + 10^{-S/10}\right)$$

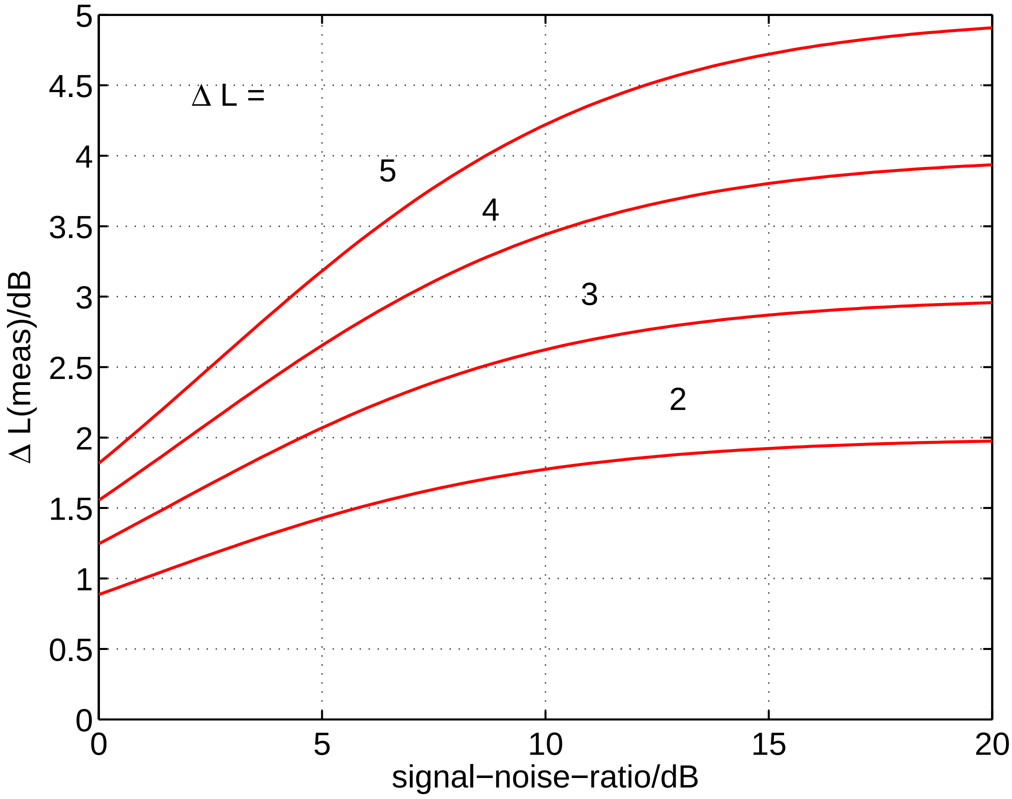

Fig. 1.11: Measured improvement $\Delta L(meas)$ versus signal-to-noise-ratio for different true improvements ΔL

Summary

Desired is an instrument 'listening' in a certain, adjustable direction:

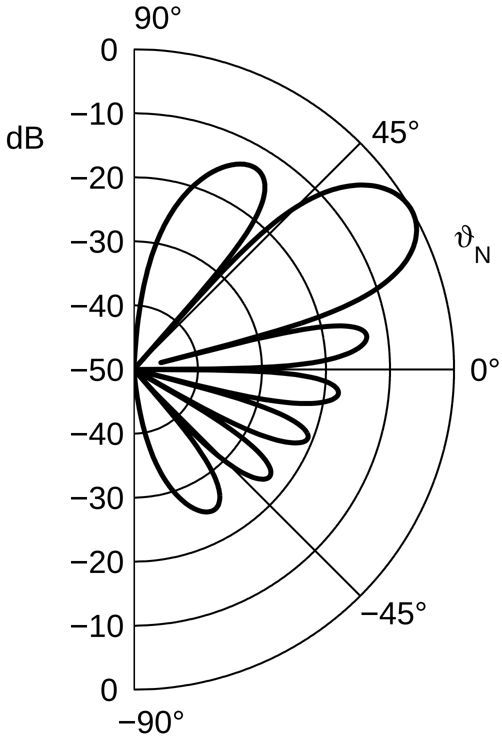

Fig. 1.12: Principle of desired directivity pattern)

Directivity pattern should have
small mainlobe for source location and
high sidelobe-mainlobe-distance for high S/N-ratio

1.3 Fundamental solution: The line-array

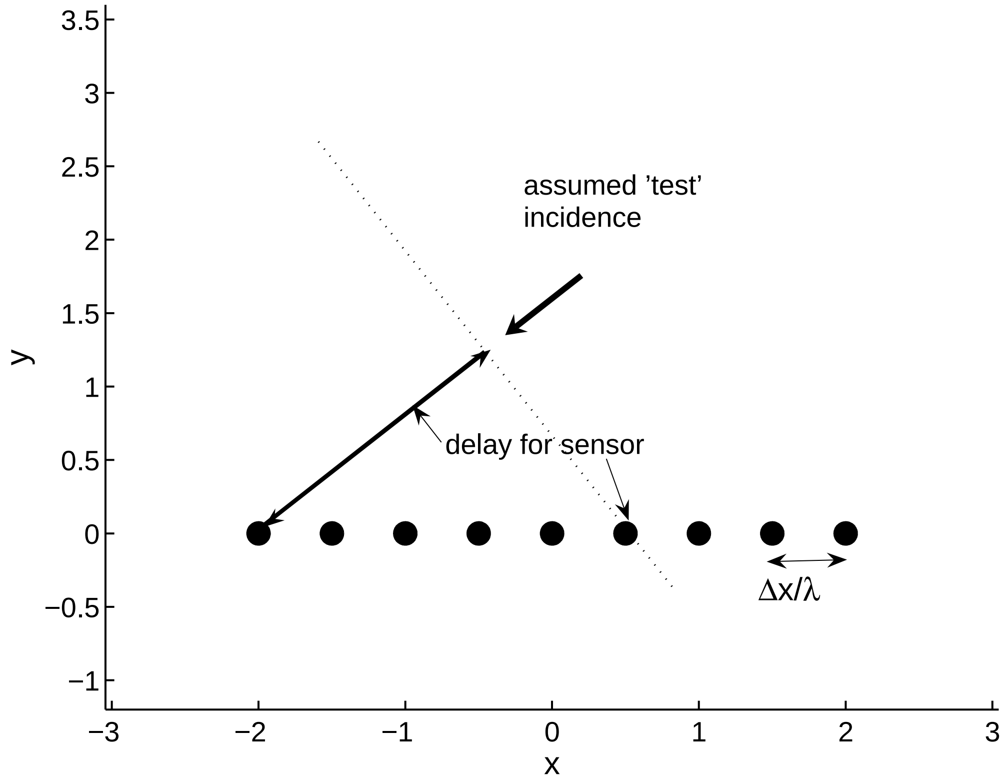

Fig. 1.13: Array setup and sensor signal delay for the algorithm 'delay and sum'

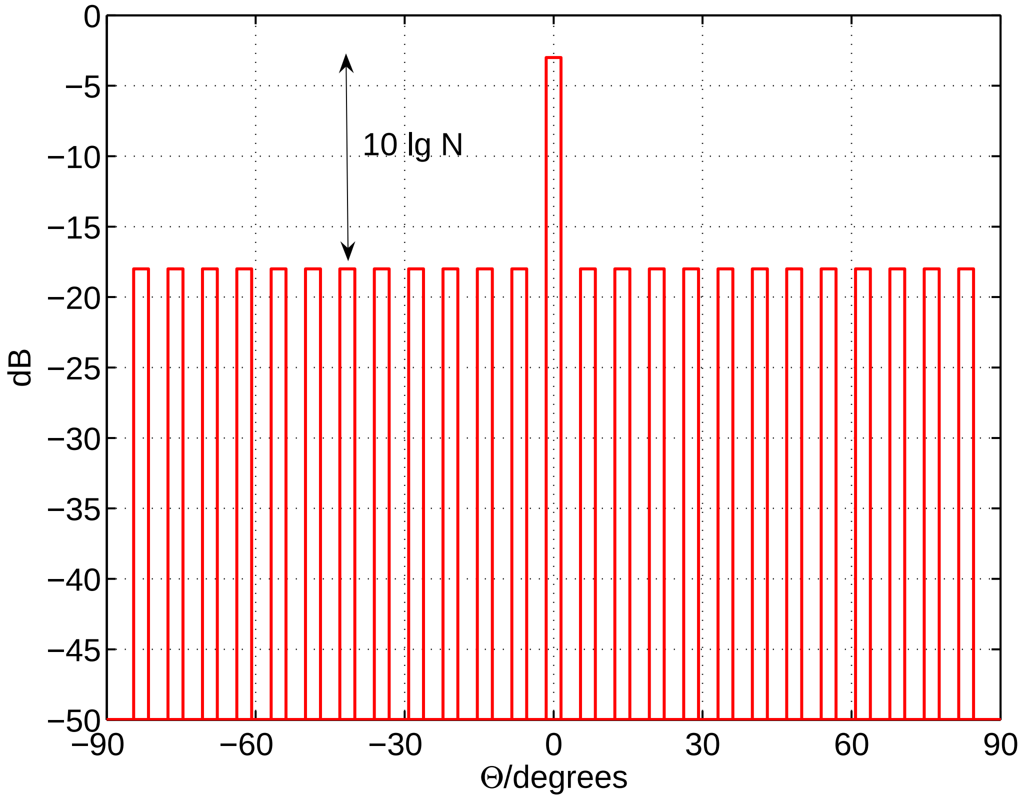

Fig. 1.14: Directivity pattern for a 'short' signal (normal incidence, principal sketch), N=number of sensors

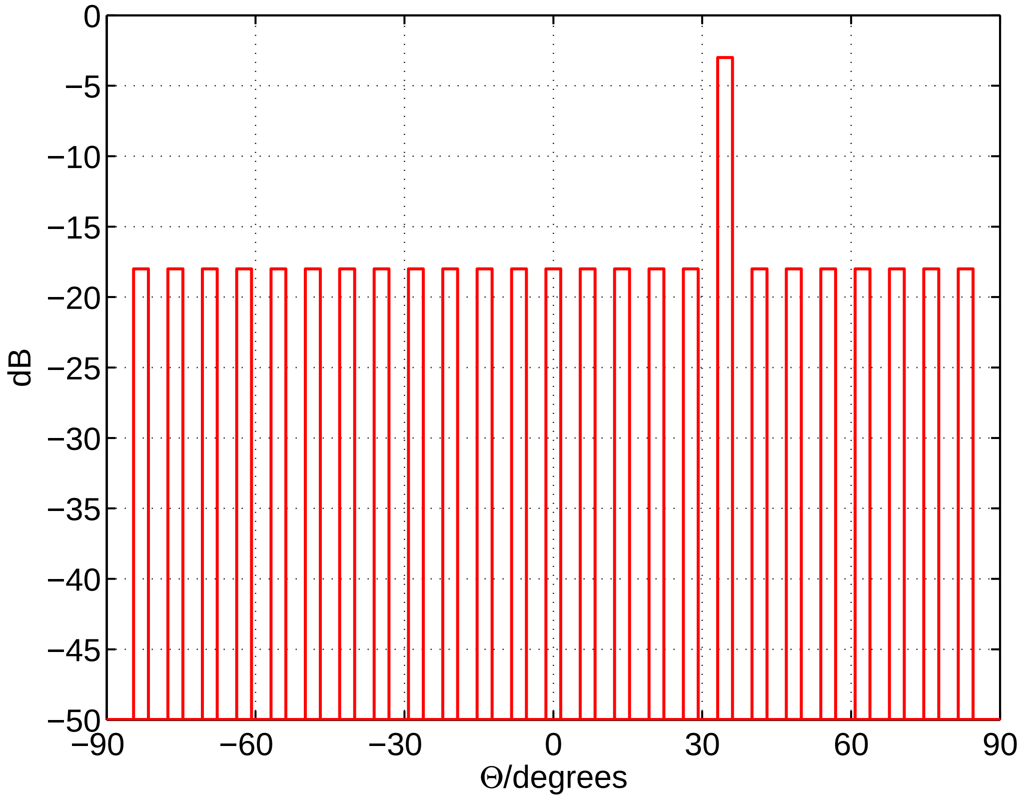

Fig. 1.15: Directivity pattern for a 'short' signal (oblique incidence, principal sketch), N=number of sensors

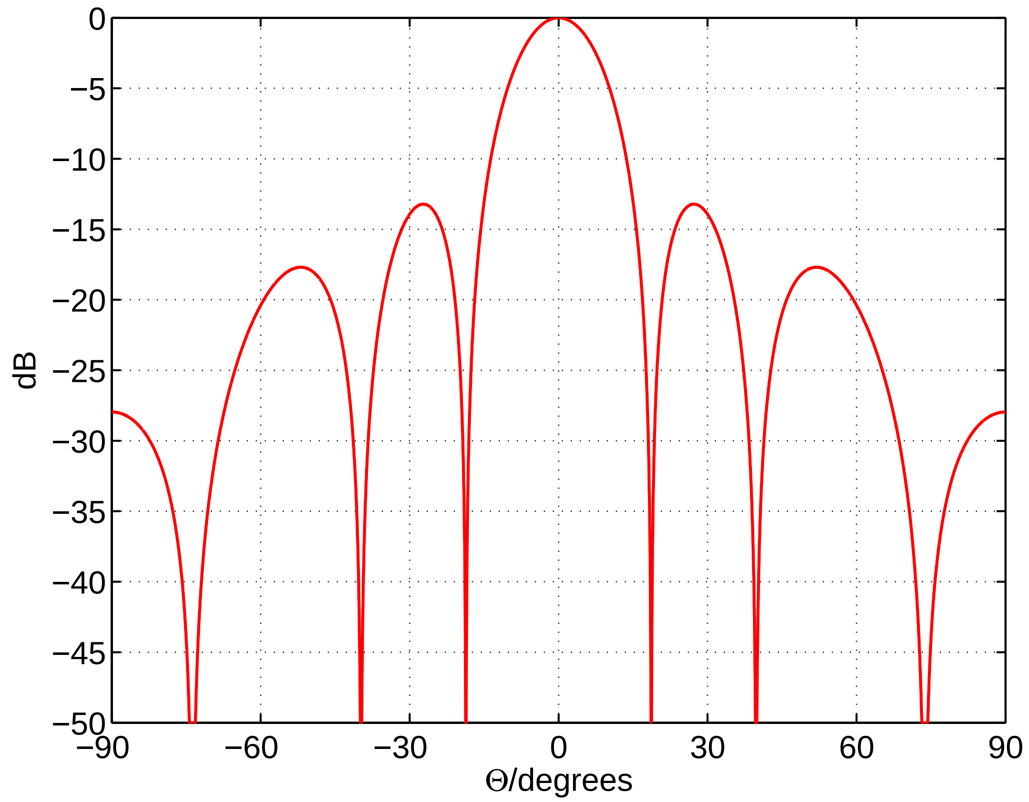

Fig. 1.16: Measured directivity pattern for a pure tone (normal incidence, $\Delta x/\lambda = 0.125$, N=25)

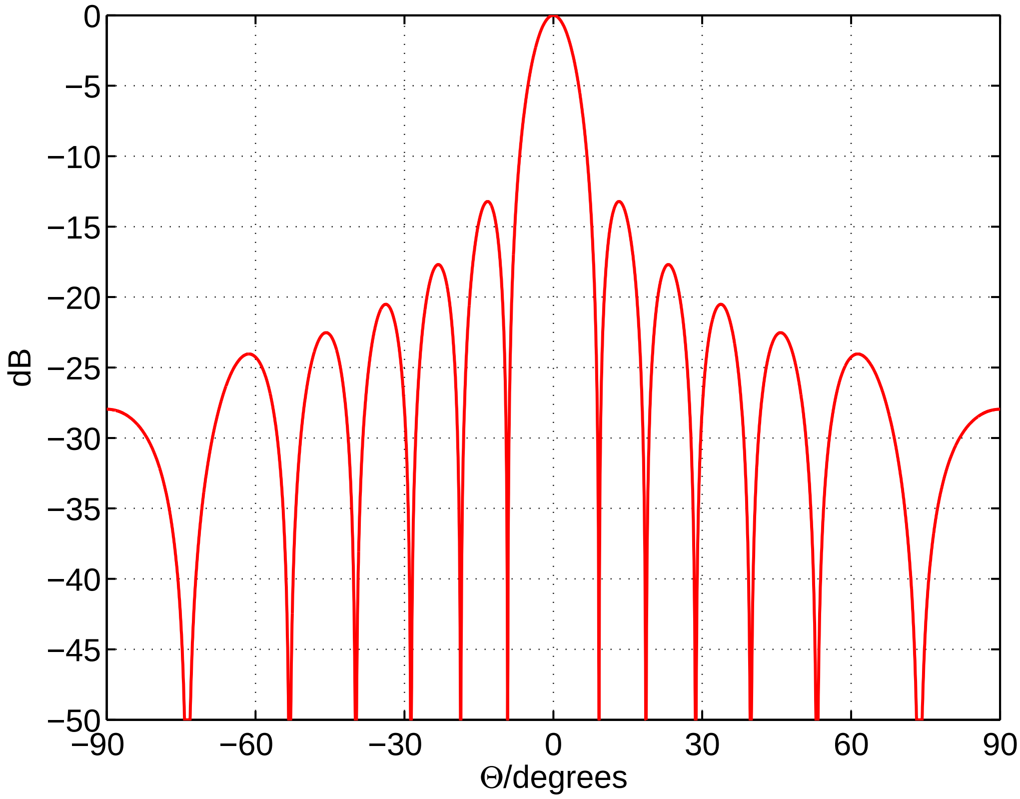

Fig. 1.17: Measured directivity pattern for a pure tone (normal incidence, $\Delta x/\lambda = 0.25$, N=25)

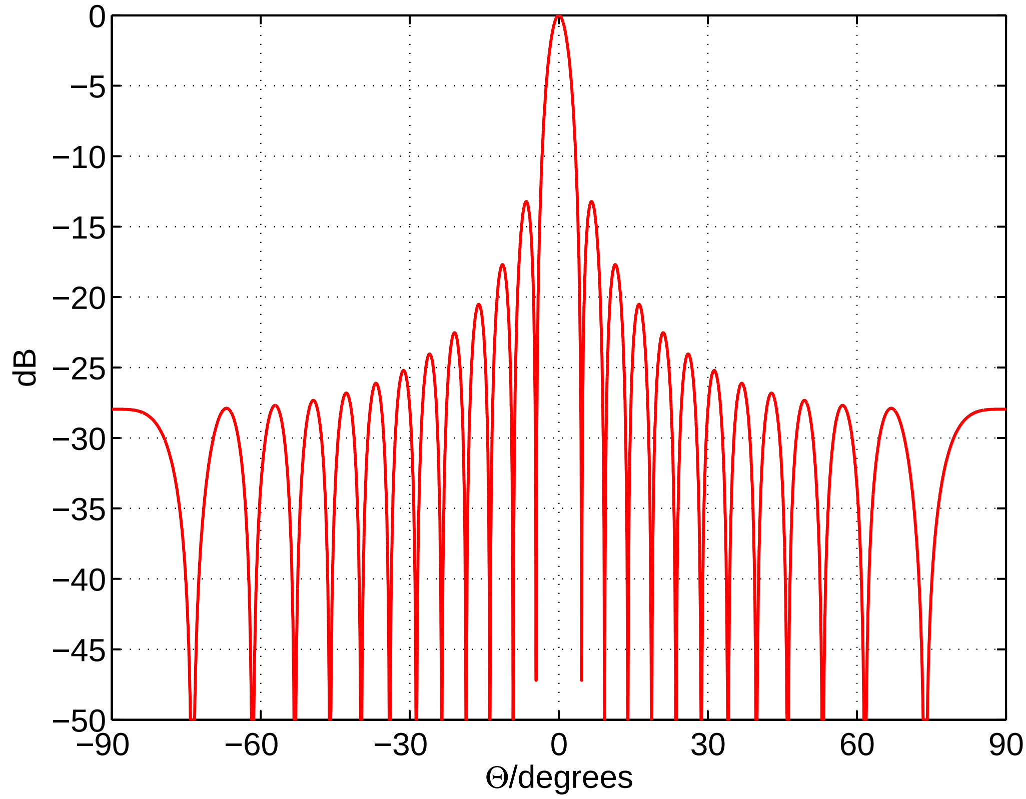

Fig. 1.18: Measured directivity pattern for a pure tone (normal incidence, $\Delta x/\lambda = 0.5$, N=25)

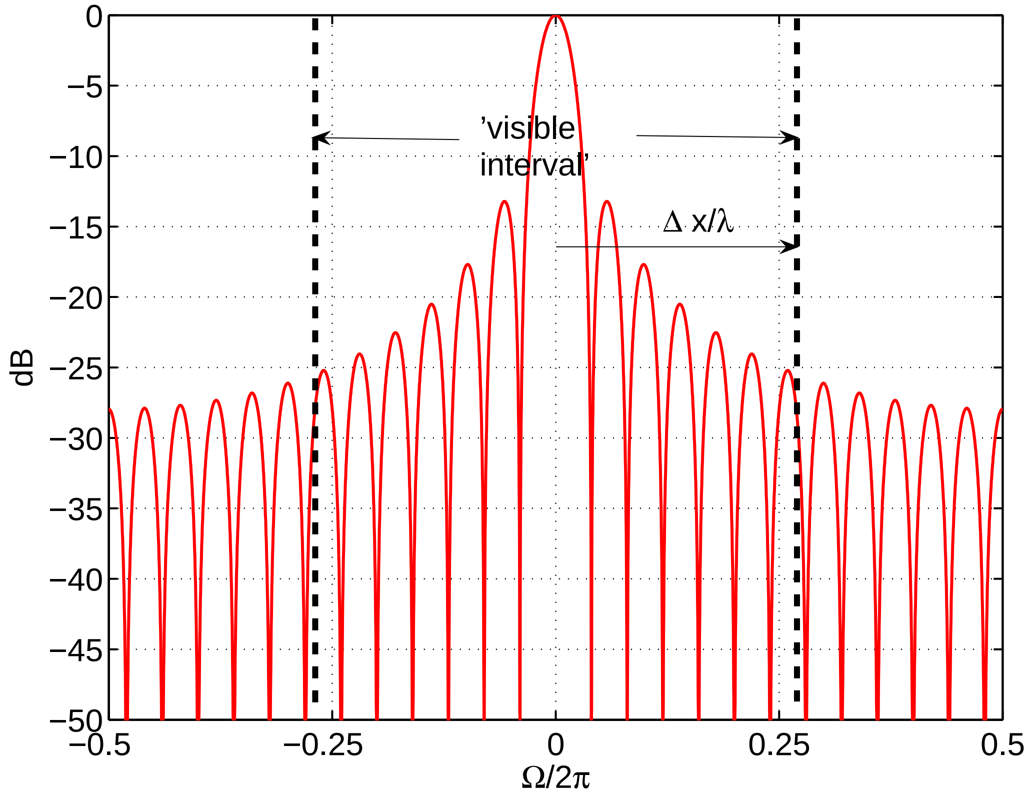

Fig. 1.19: Wavenumber spectrum calculated from the microphone signals. Directivity pattern = some distorted interval of wavenumber spectrum

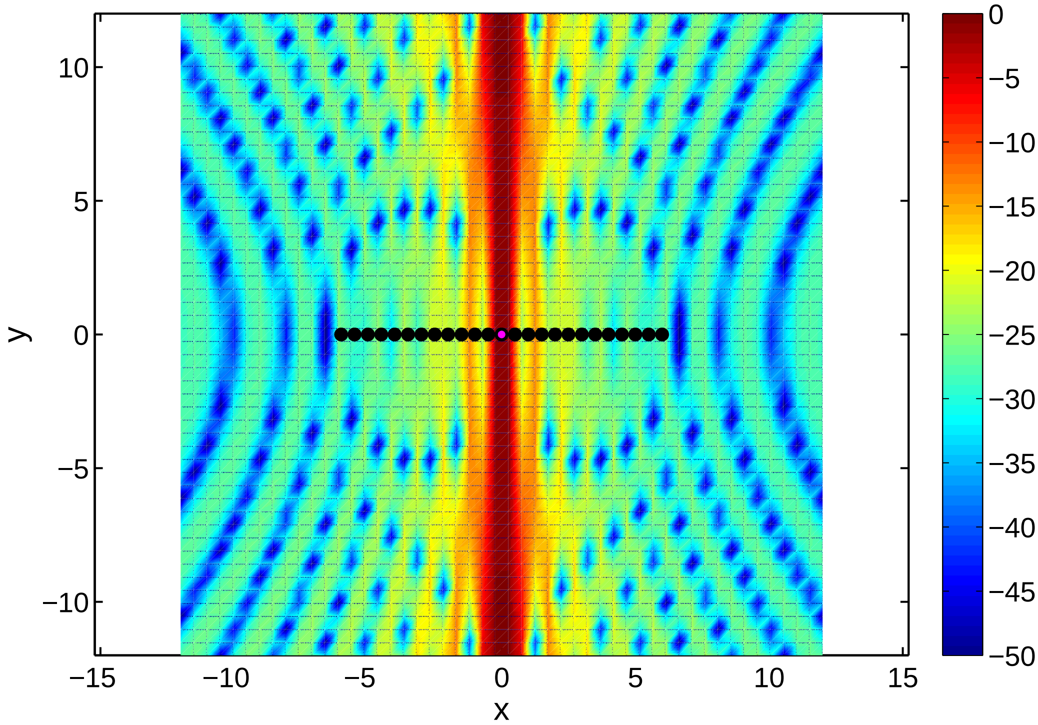

Fig. 1.20: Colorplot (like a photo) of the array output $\Delta x/\lambda = 0.5$, normal incidence (N=25)

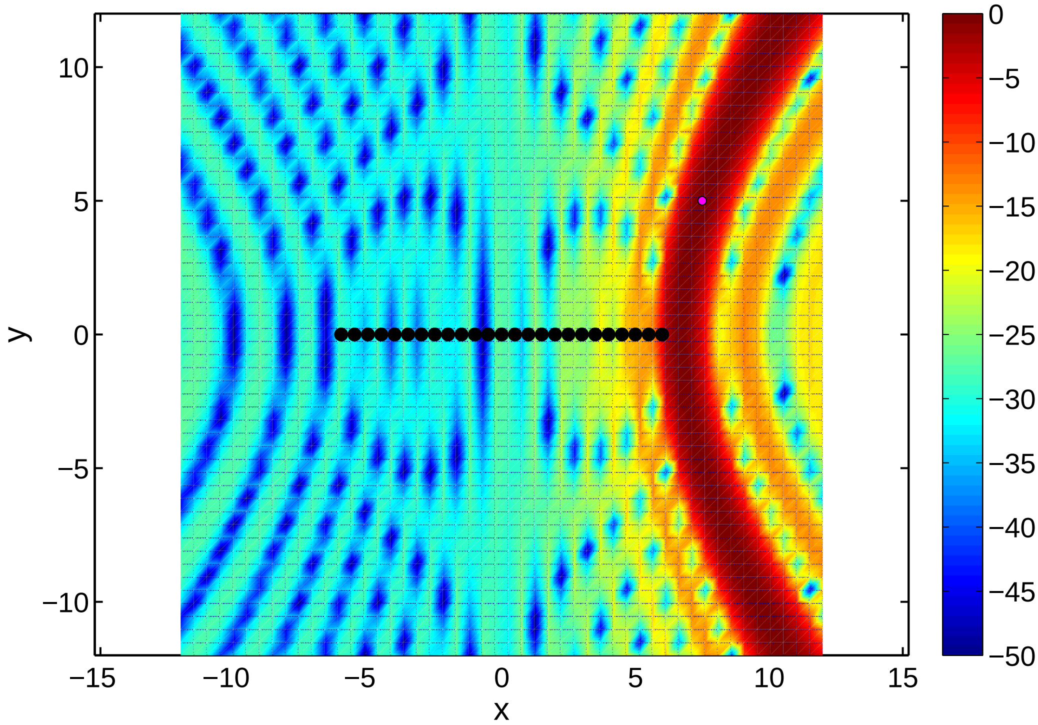

Fig. 1.21: Colorplot (like a photo) of the array output $\Delta x/\lambda = 0.5$, oblique incidence (N=25)

Part 2

Weights and windows (beamforming)

In principle: wavenumber spectrum is calculated from the (complex) amplitude sequence

$\mapsto$ Technique of 'weights and windows' for time series can be applied to 'form the beam' and to manipulate the 'mainlobe-sidelobe-distance'

Examples: Rectangular (see before), Hanning, Dolp-Chebyshev (and others: for example Kaiser-Bessel, Flat-Top, Hamming)

2.1 Role of specific window

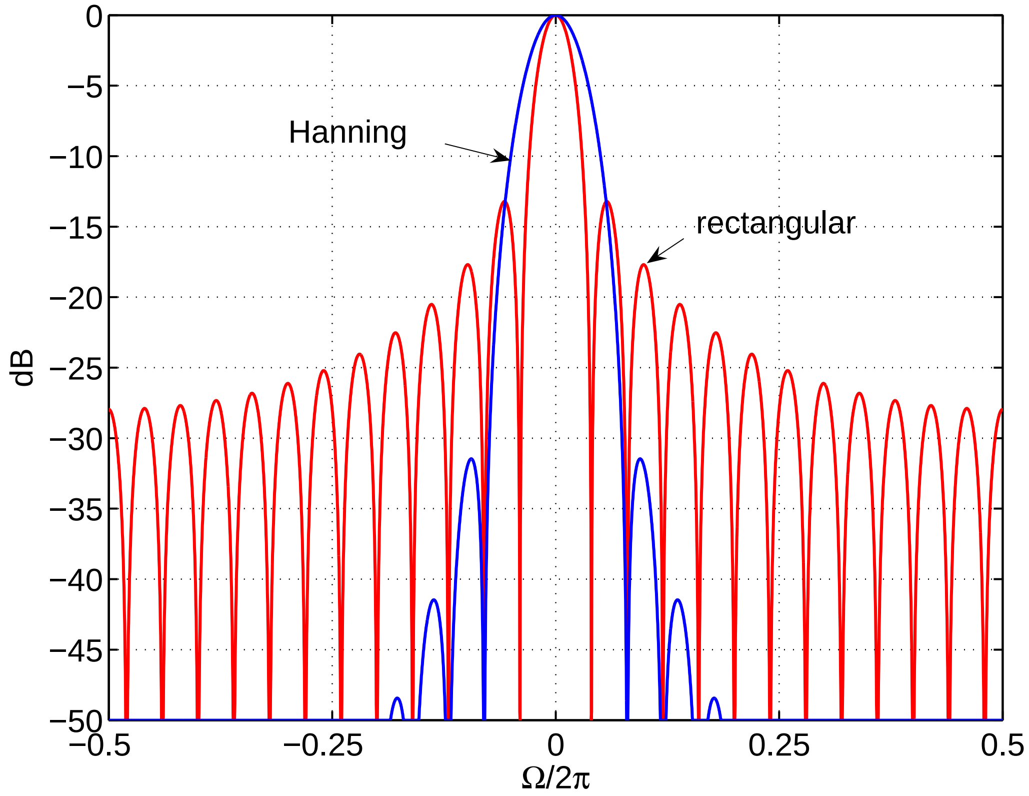

Fig. 2.1: Wavenumber spectra for rectangular and for Hanning (cos^2) window (N=25)

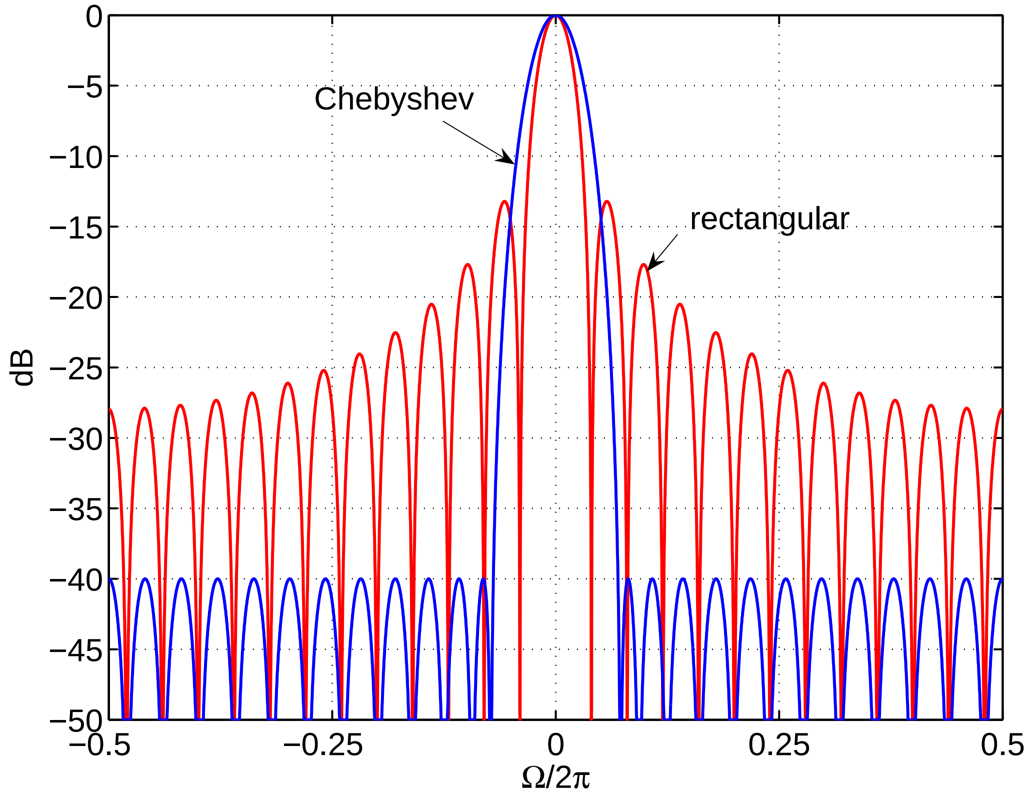

Fig. 2.2: Wavenumber spectra for rectangular and Dolph-Chebyshev window (N=25)

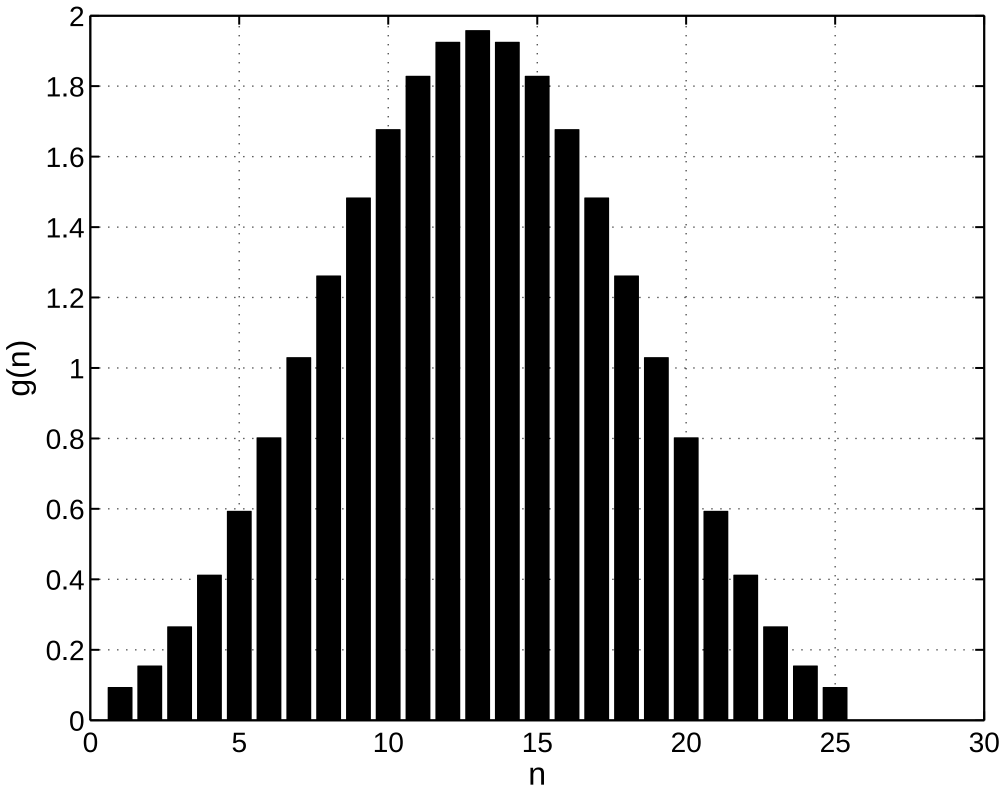

Fig. 2.3: Dolph-Chebyshev window itself (N=25, distance=50 dB)

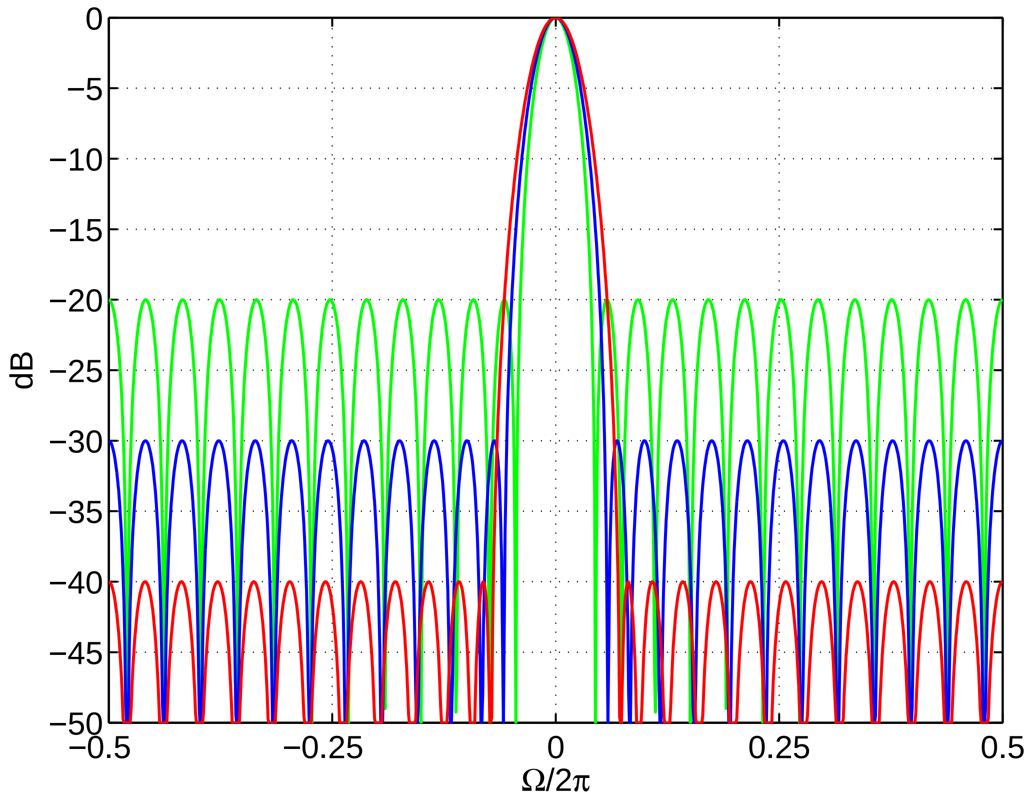

Fig. 2.4: Wavenumber spectra for different Dolph-Chebyshev windows

2.2 Construct your own window!

Form of wavenumberspectrum always is fixed by the distribution of zeros:

$\mapsto$ Choosing a zeros pattern allows to install a certain desired structure of mainlobe-width and mainlobe-sidelobe-distance

2.3 Role of calibration

Uncalibrated array output = sum of 'true' amplitude series and spatially white noise

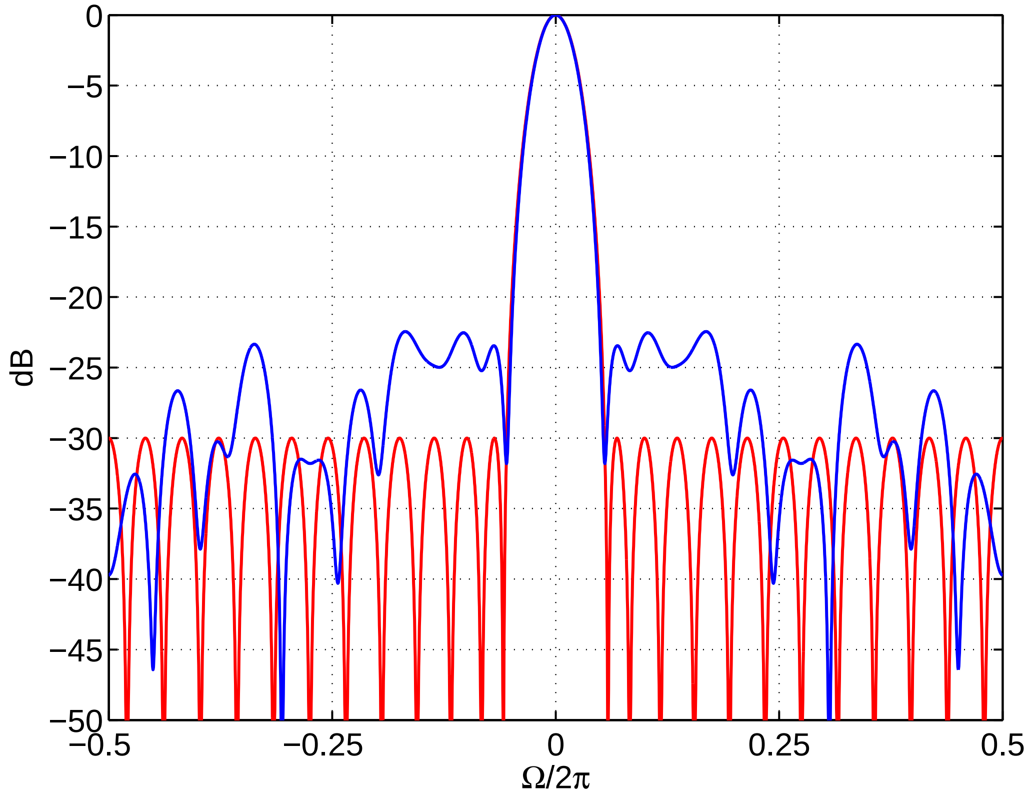

Fig. 2.5: Wavenumber spectrum for calibrated (red) and for uncalibrated (blue) array. Dolph-Chebyshev window used with mainlobe-sidelobe-distance = 30 dB (mean calibration error 1 dB)

Part 3

Layout of array geometry

3.1 Sensor distribution along a line

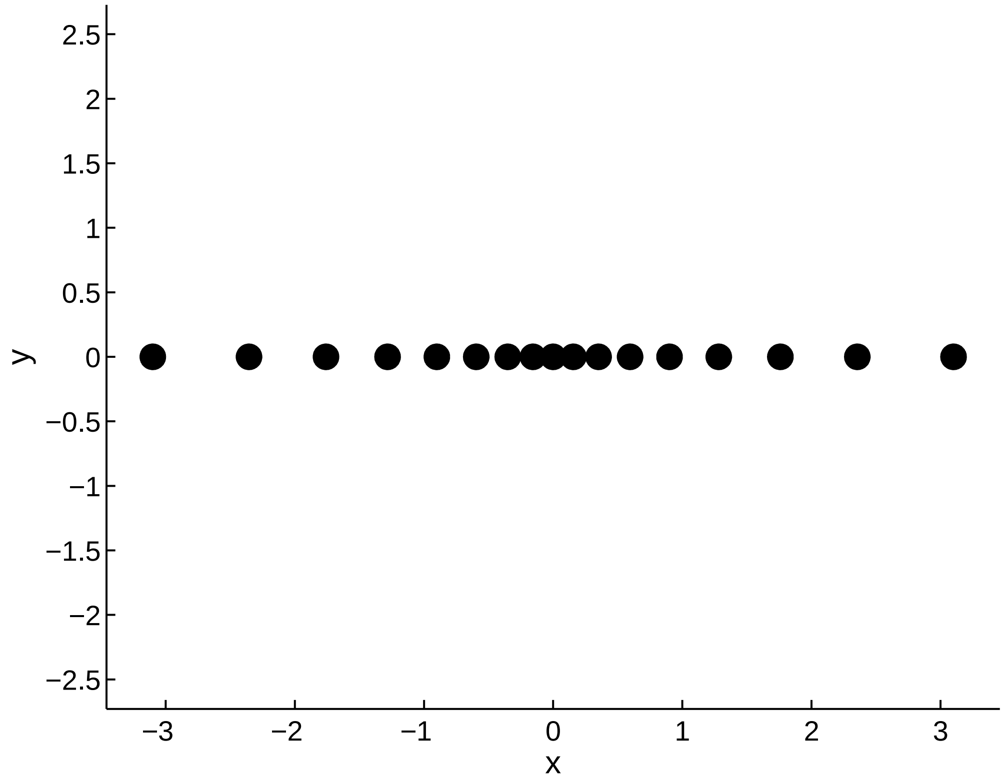

Fig. 3.1: Setup of exponential array

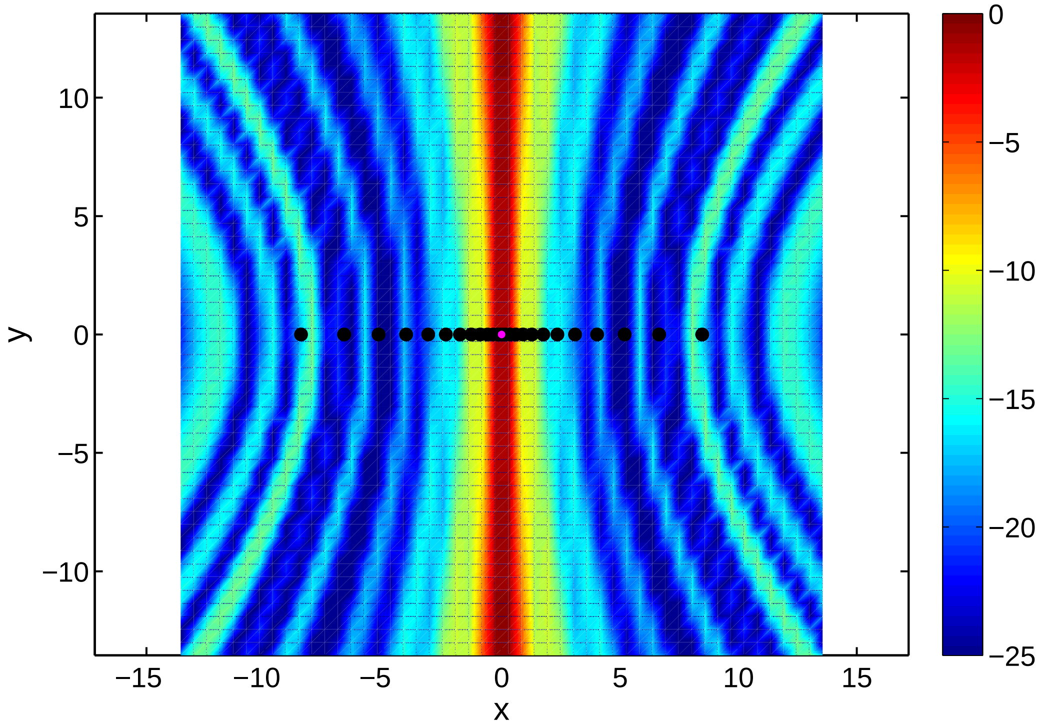

Fig. 3.2: Colorplot of the EXPONENTIAL array output $\Delta x/\lambda = 0.125$, normal incidence (N=25)

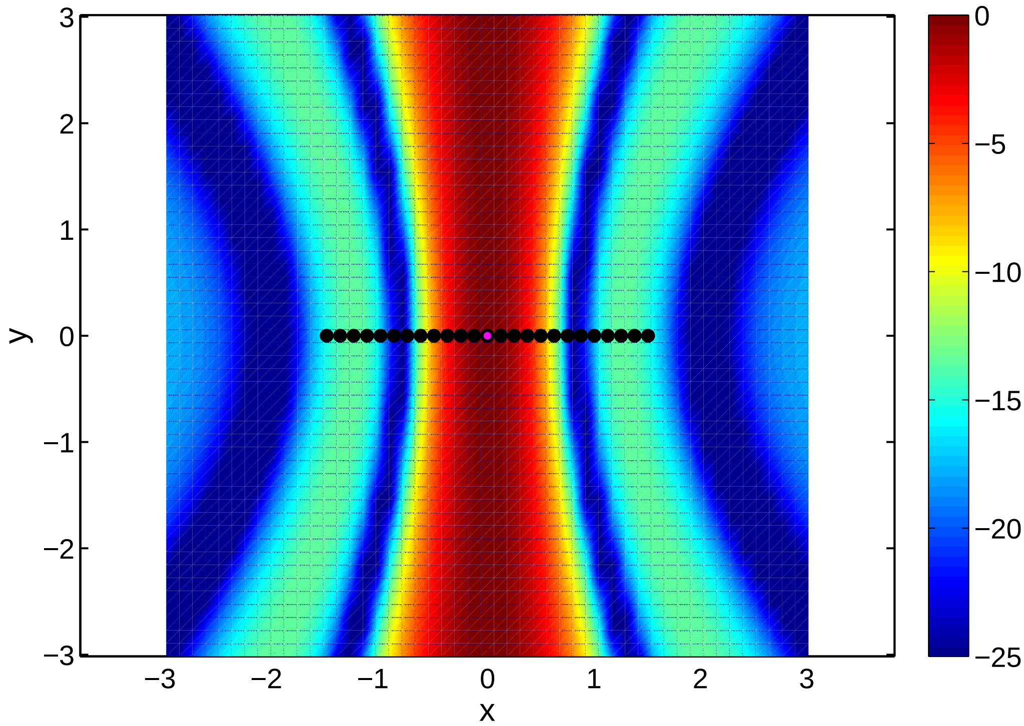

Fig. 3.3: Colorplot of the EQUIDISTANT array output $\Delta x/\lambda = 0.125$, normal incidence (N=25)

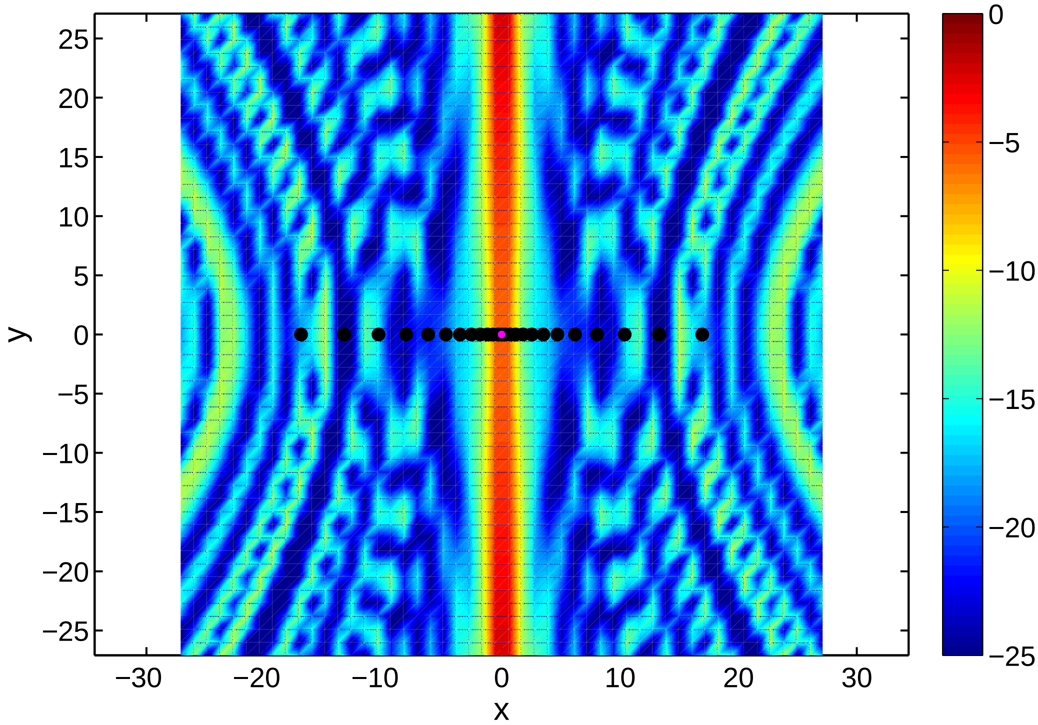

Fig. 3.4: Colorplot of the EXPONENTIAL array output $\Delta x/\lambda = 0.25$, normal incidence (N=25)

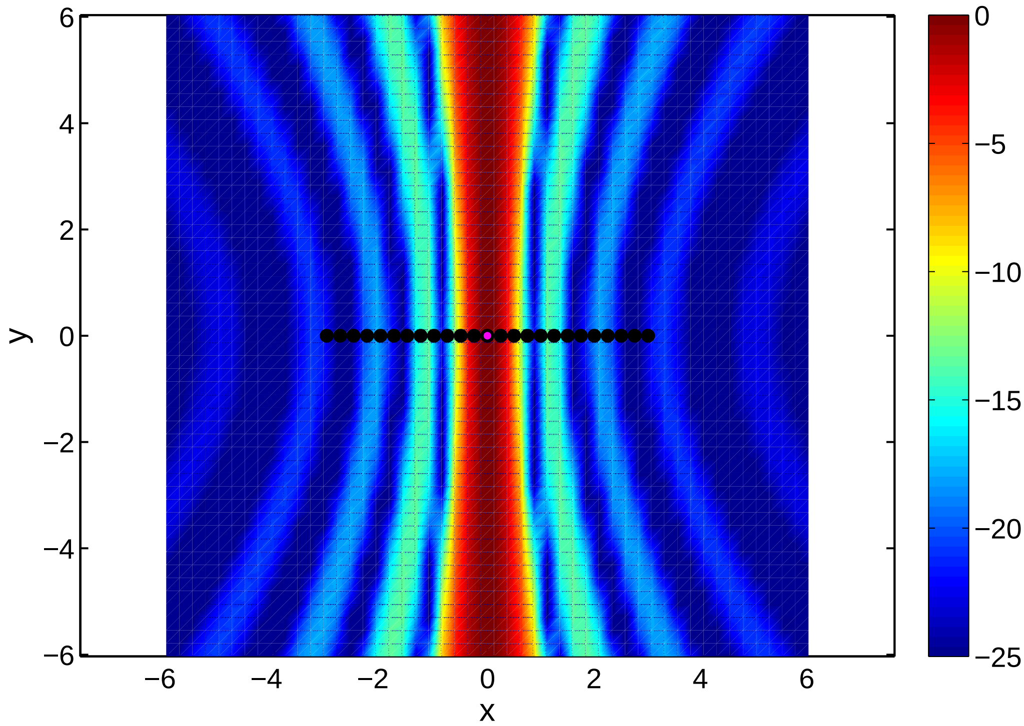

Fig. 3.5: Colorplot of the EQUIDISTANT array output $\Delta x/\lambda = 0.25$, normal incidence (N=25)

3.2 Sparse 2D arrays: cross and circle arrays

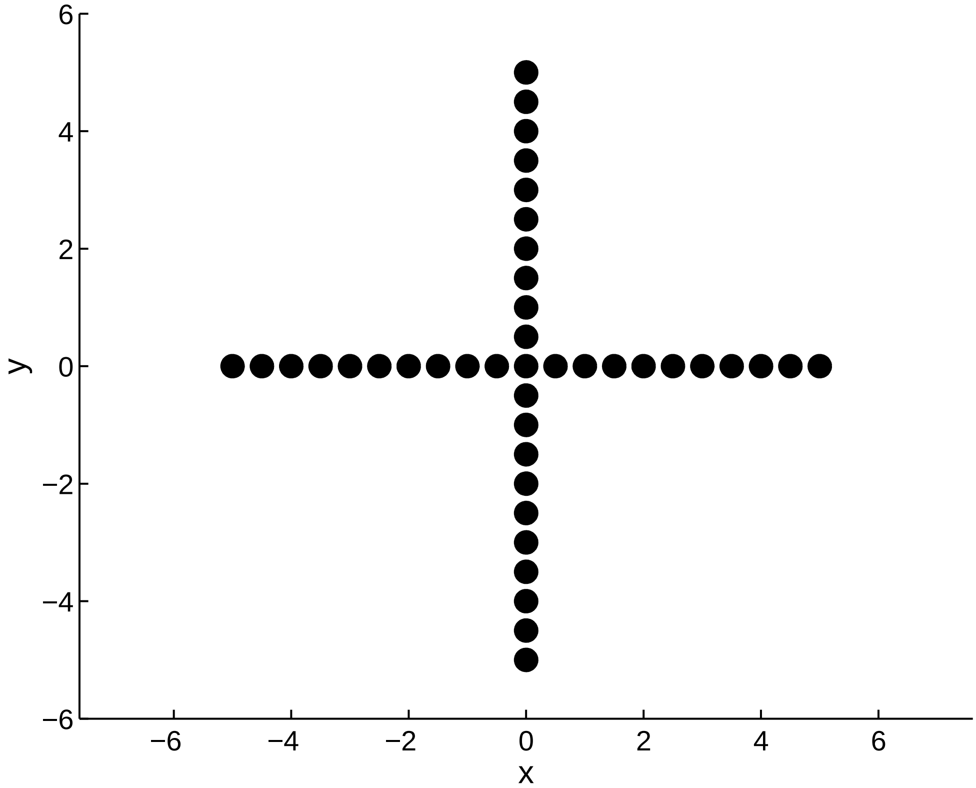

Fig. 3.6: Setup of cross array

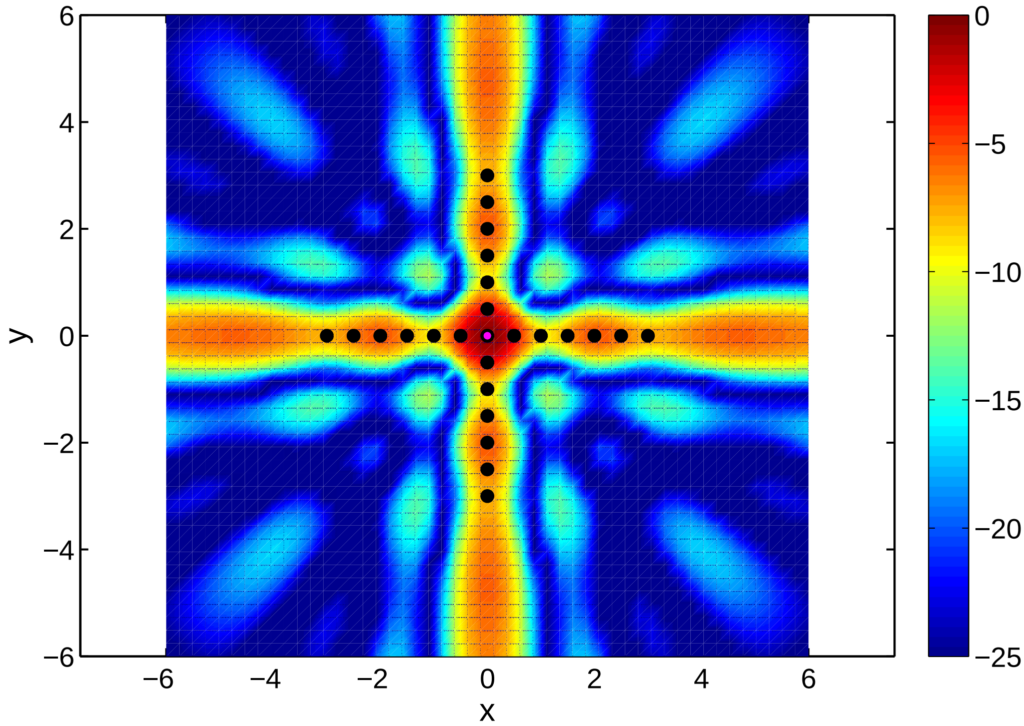

Fig. 3.7: Colorplot of the cross array output $\Delta x/\lambda = 0.5$, normal incidence (N=25)

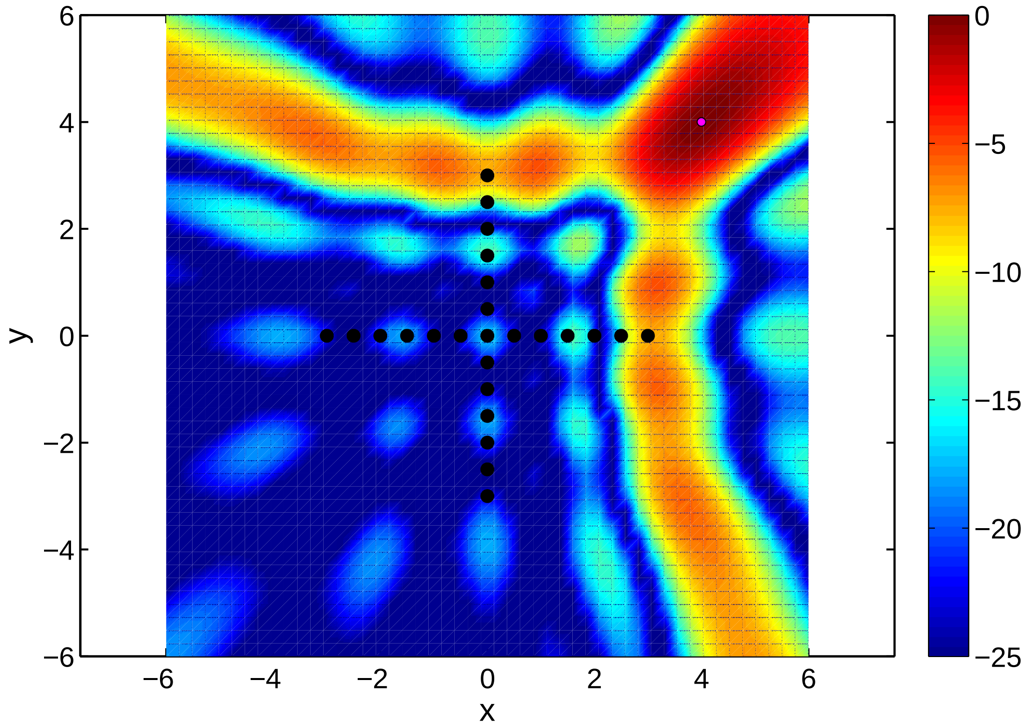

Fig. 3.8: Colorplot of the cross array output $\Delta x/\lambda = 0.5$, oblique incidence (N=25)

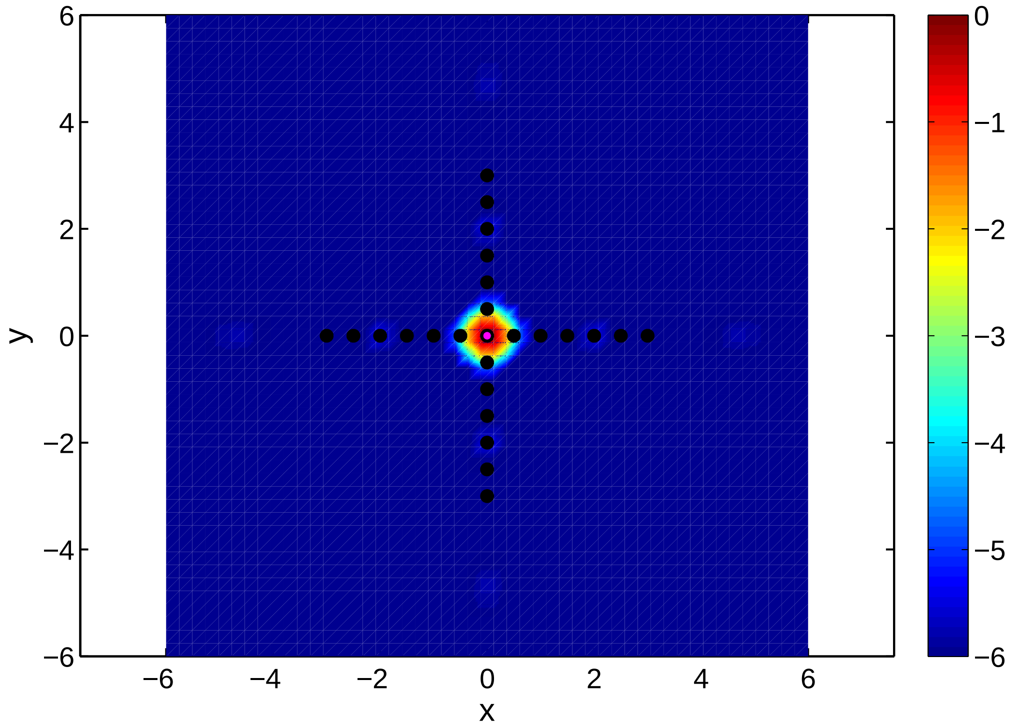

Fig. 3.9: Colorplot of the cross array output $\Delta x/\lambda = 0.5$, normal incidence (N=25), low range displayed

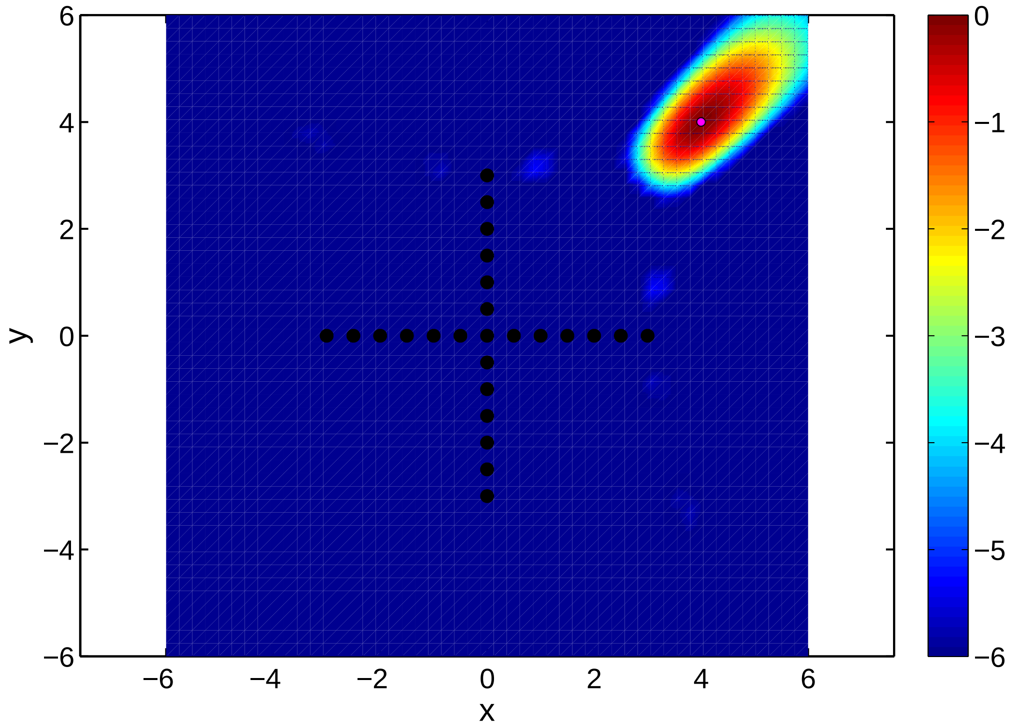

Fig. 3.10: Colorplot of the cross array output $\Delta x/\lambda = 0.5$, oblique incidence (N=25), low range displayed

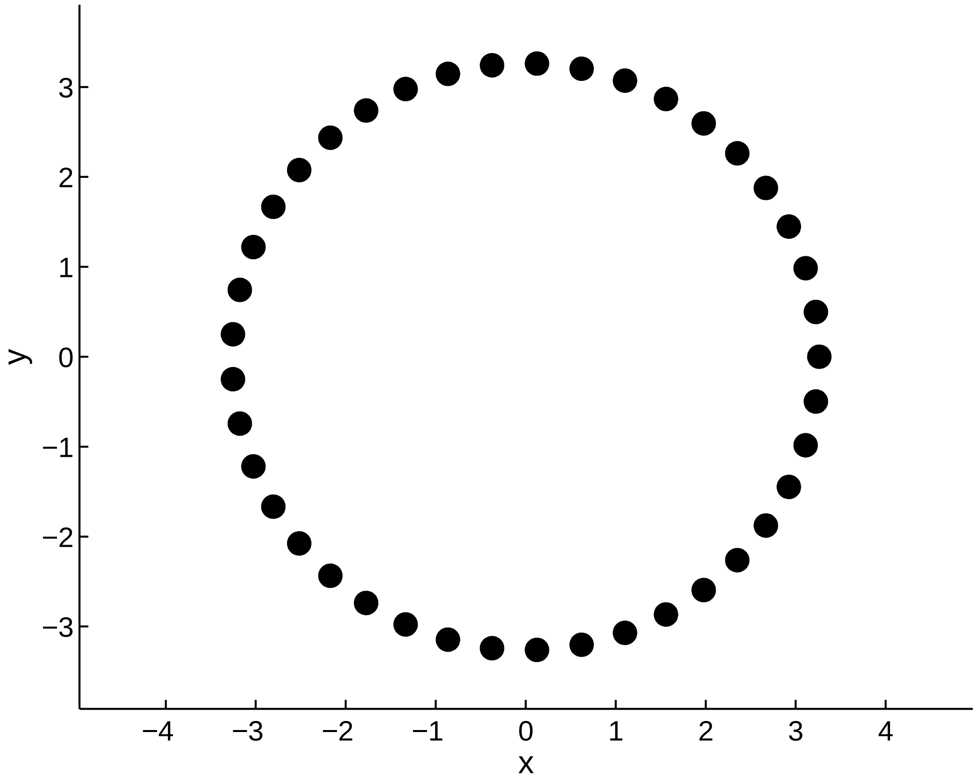

Fig. 3.11: Setup of circle array

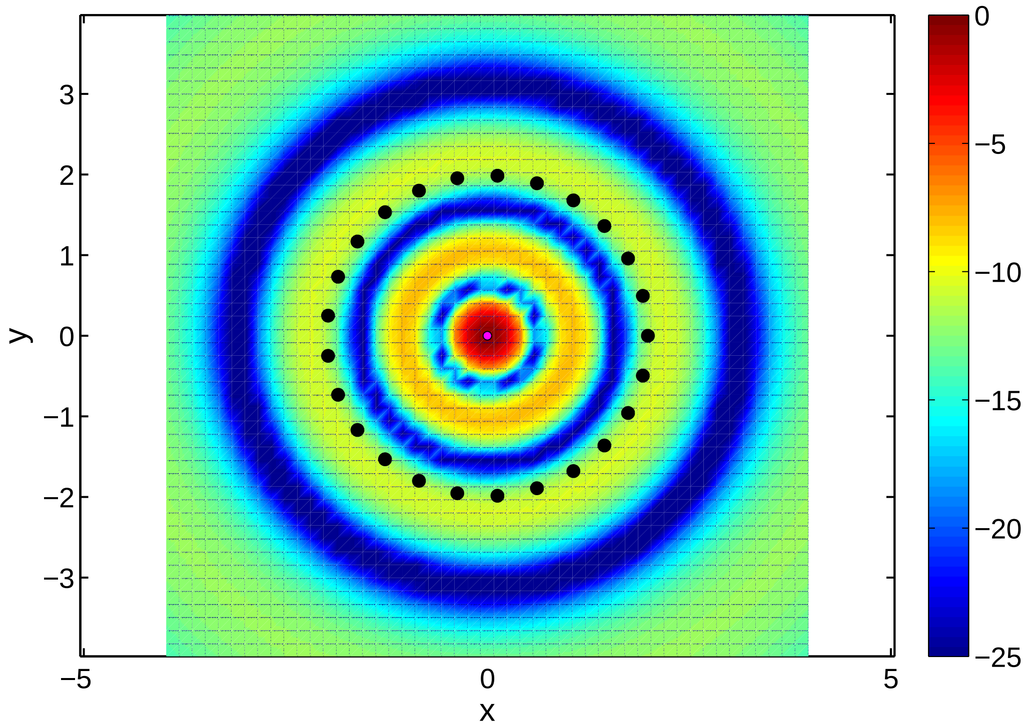

Fig. 3.12: Colorplot of the circle array output $\Delta x/\lambda = 0.5$, normal incidence (N=25)

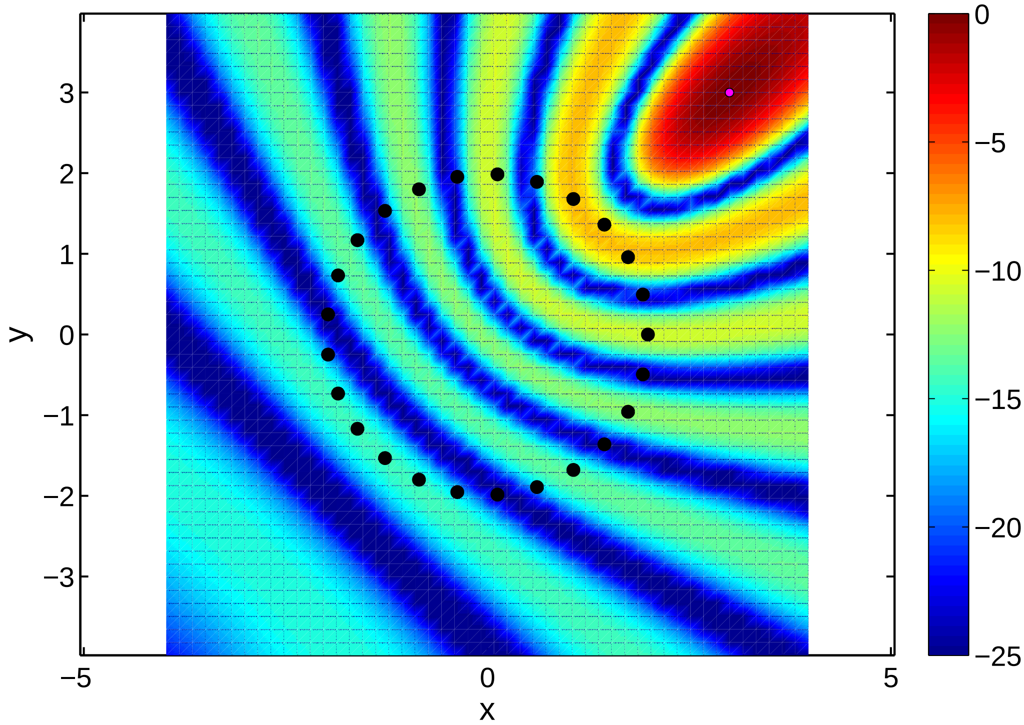

Fig. 3.13: Colorplot of the circle array output $\Delta x/\lambda = 0.5$, oblique incidence (N=25)

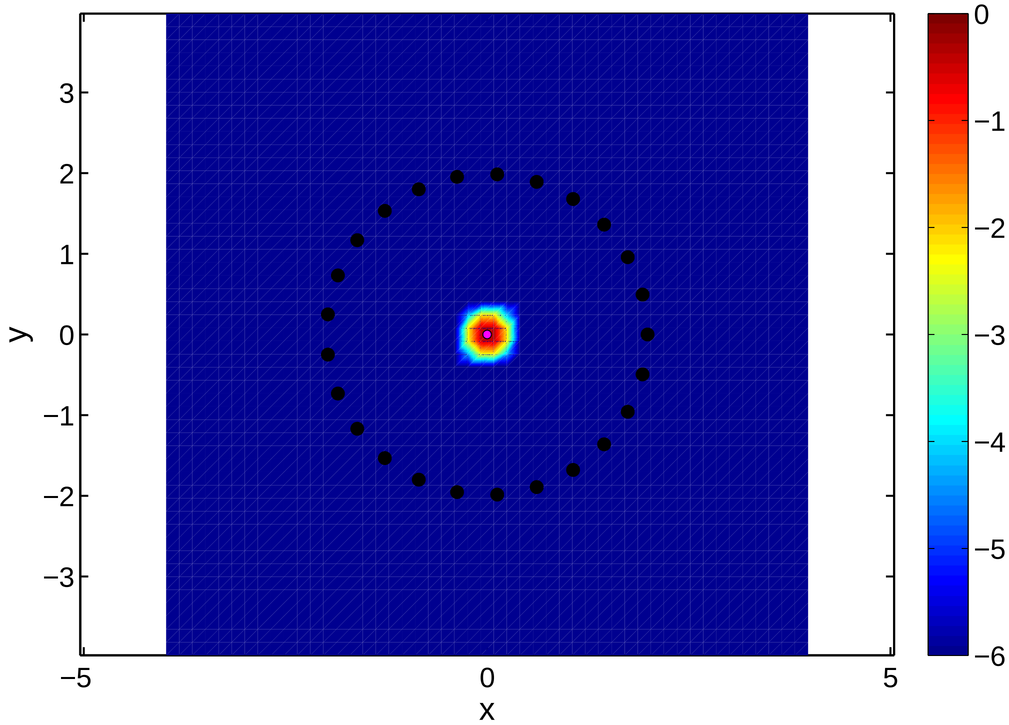

Fig. 3.14: Colorplot of the circle array output $\Delta x/\lambda = 0.5$, normal incidence (N=25), low range displayed

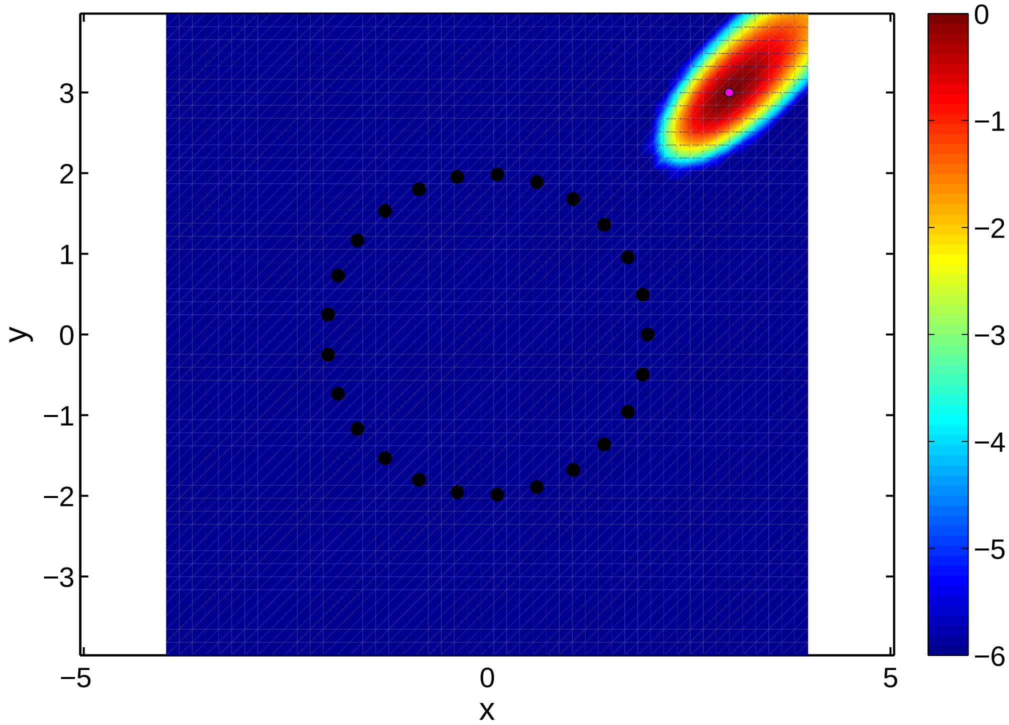

Fig. 3.15: Colorplot of the circle array output $\Delta x/\lambda = 0.5$, oblique incidence (N=25), low range displayed

3.3 'Dense' 2D arrays: quadratic array

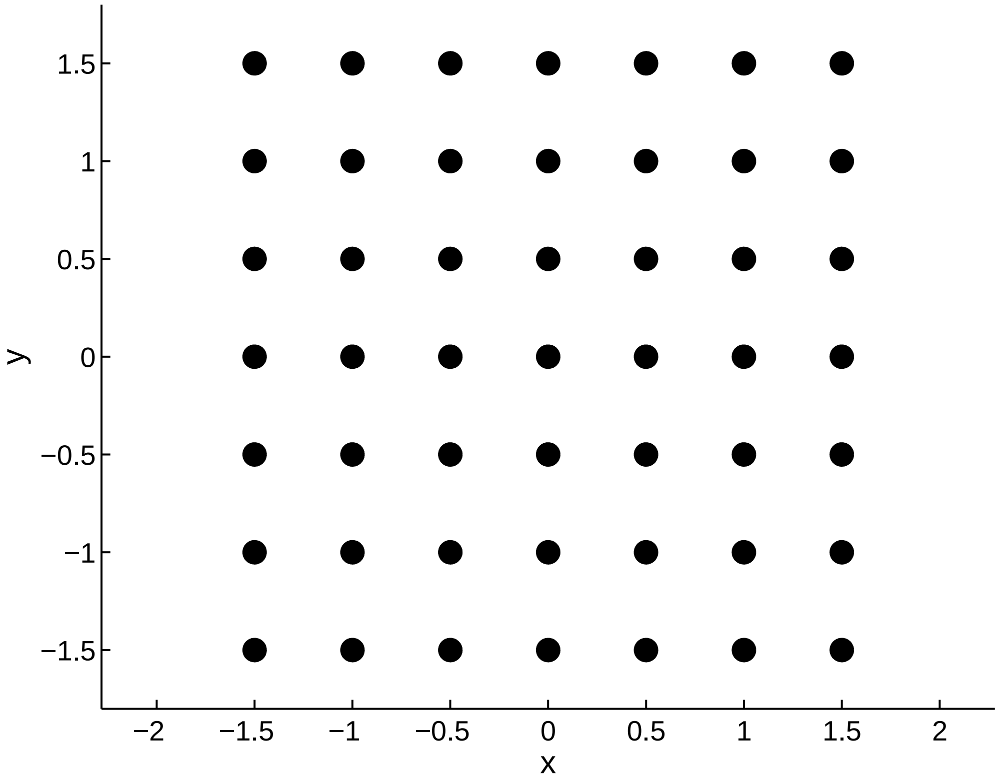

Fig. 3.16: Setup of quadratic array

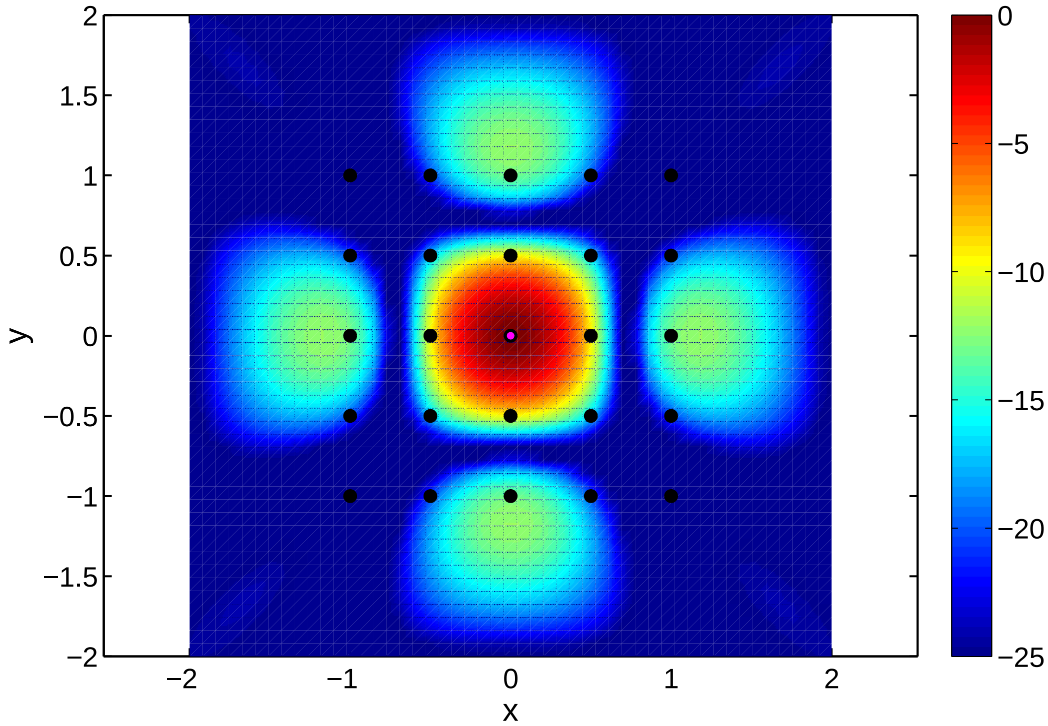

Fig. 3.17: Colorplot of the quadratic array output $\Delta x/\lambda = 0.5$, normal incidence (N=25)

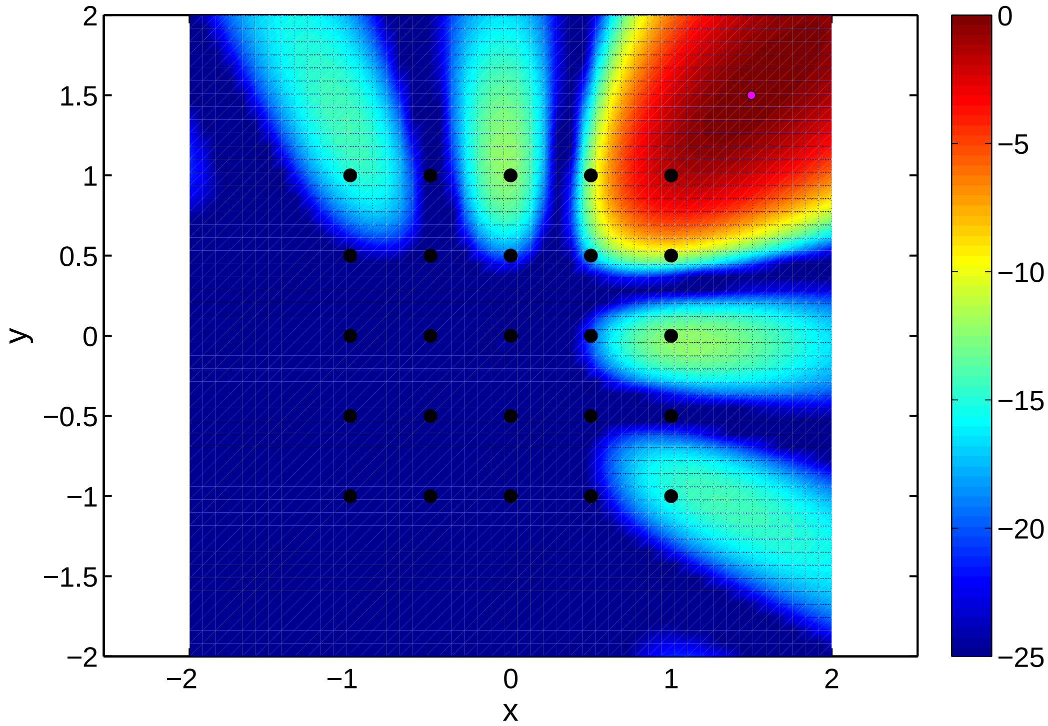

Fig. 3.18: Colorplot of the quadratic array output $\Delta x/\lambda = 0.5$, oblique incidence (N=25)

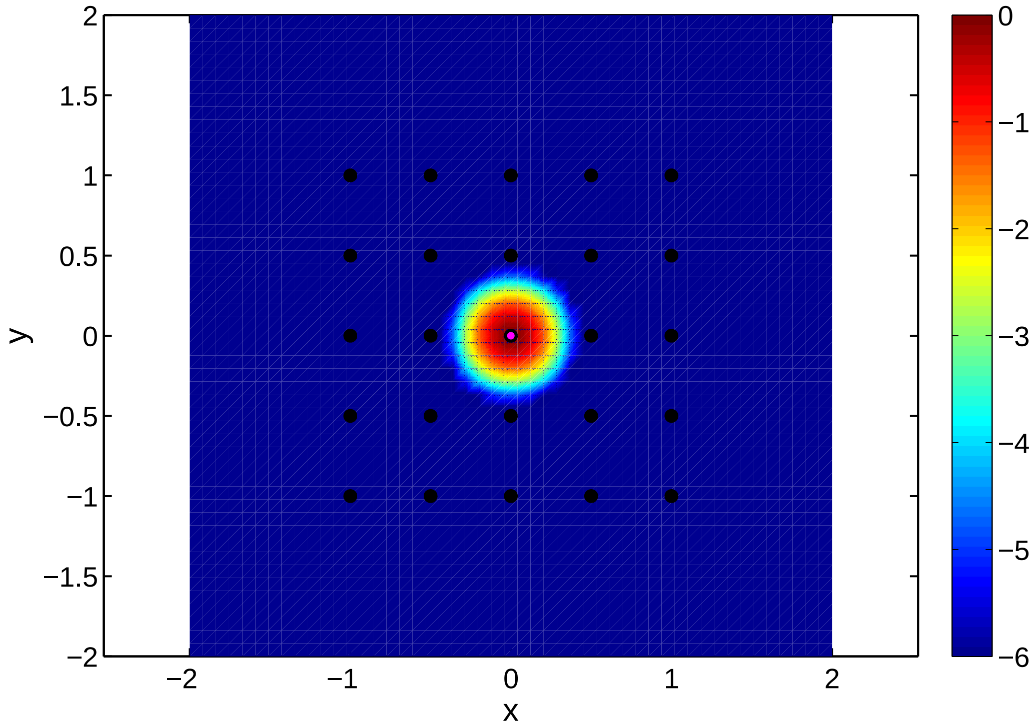

Fig. 3.19: Colorplot of the quadratic array output $\Delta x/\lambda = 0.5$, normal incidence (N=25), low range displayed

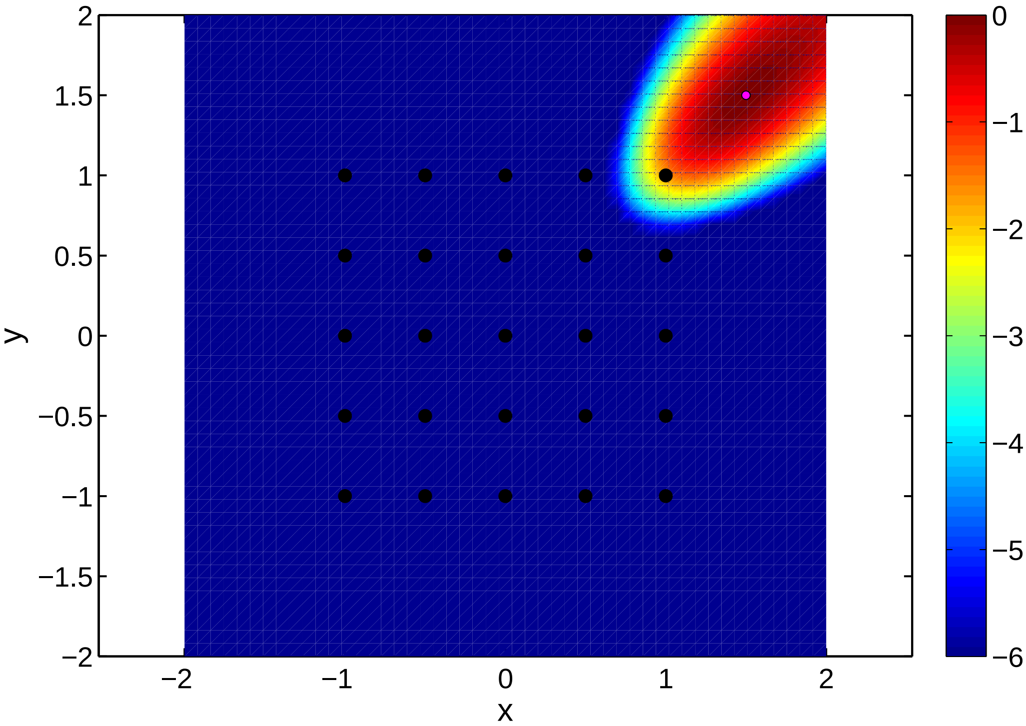

Fig. 3.20: Colorplot of the quadratic array output $\Delta x/\lambda = 0.5$, oblique incidence (N=125), low range displayed

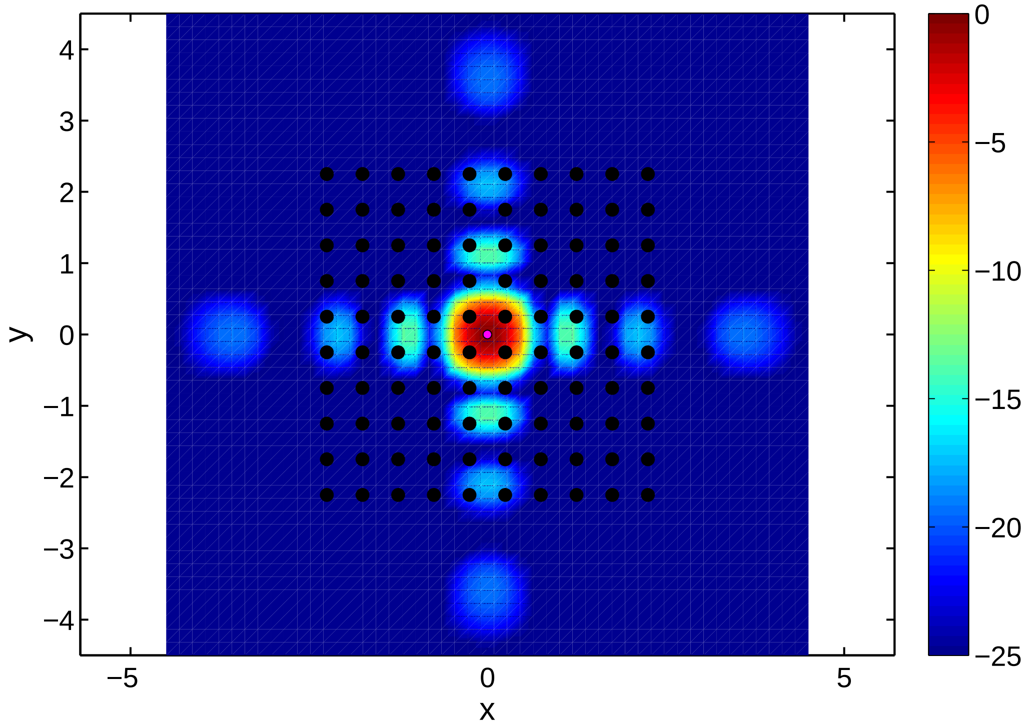

Fig. 3.21: Colorplot of the quadratic array output $\Delta x/\lambda = 0.5$, normal incidence (N=100)

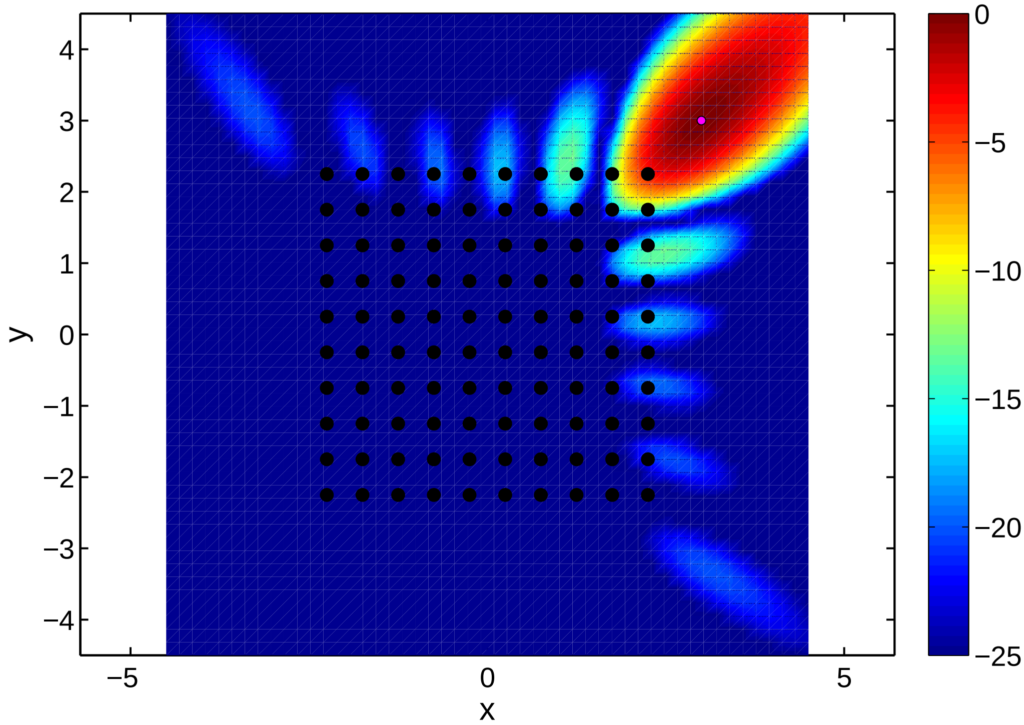

Fig. 3.22: Colorplot of the quadratic array output $\Delta x/\lambda = 0.5$, oblique incidence (N=100)

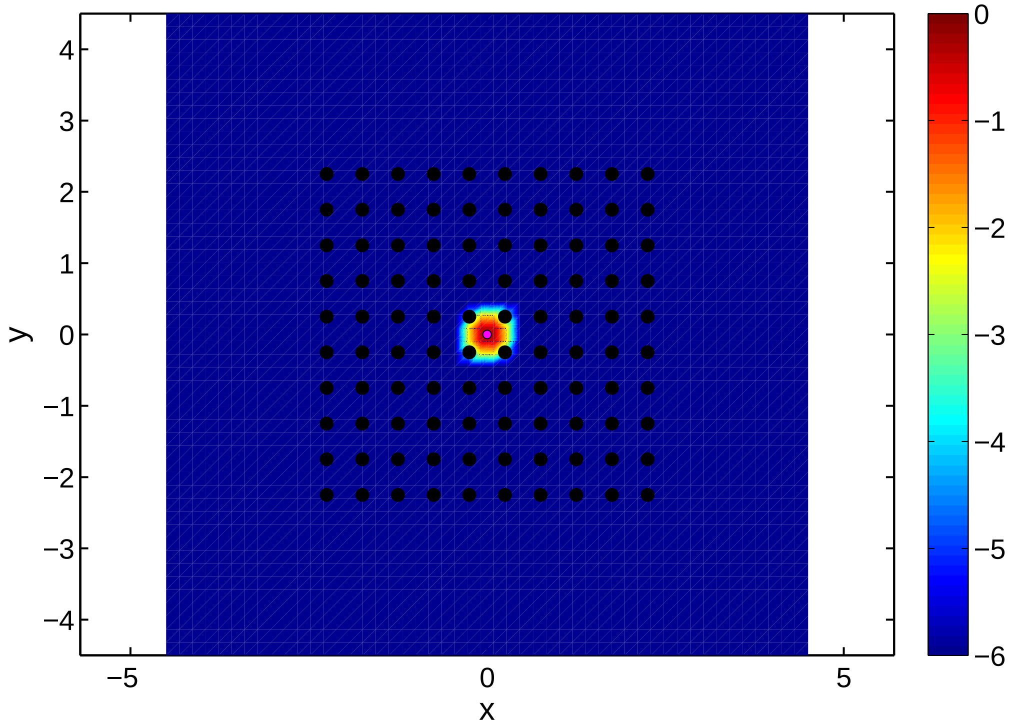

Fig. 3.23: Colorplot of the quadratic array output $\Delta x/\lambda = 0.5$, normal incidence (N=100), low range displayed

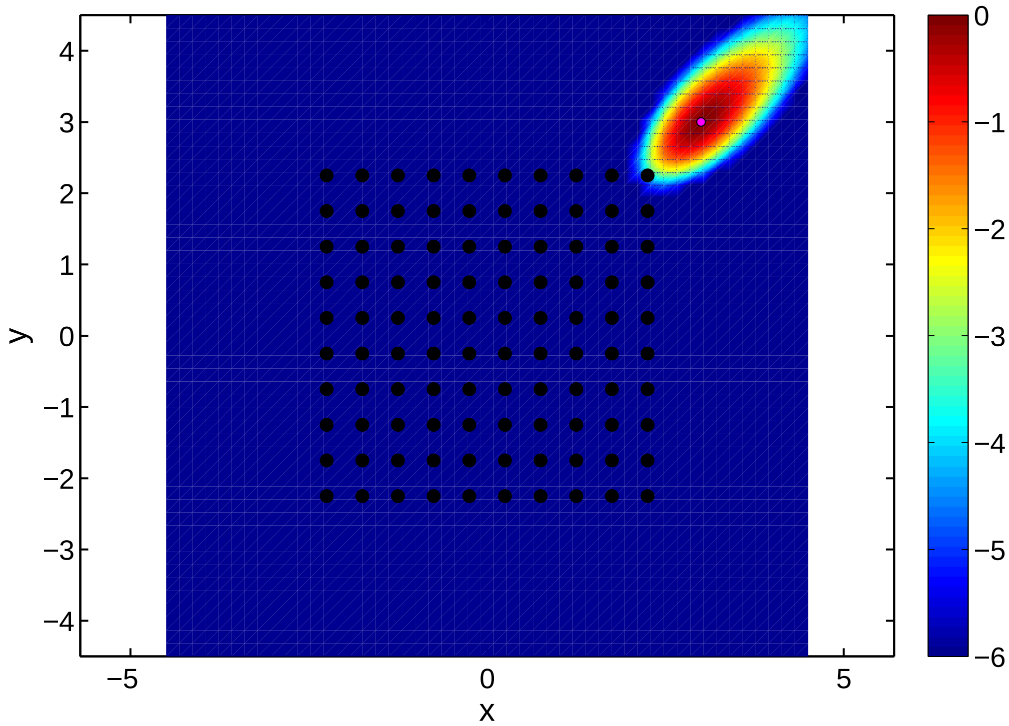

Fig. 3.24: Colorplot of the quadratic array output $\Delta x/\lambda = 0.5$, oblique incidence (N=100), low range displayed

Part 4

Alternative beamforming method: 'modern' spectral estimation

4.1 The 'all-zeros' (MA) approach

polynomial shape = product of all distances from current point x to all zeros x_i

$$|P(x)| = \prod |x - x_i|$$

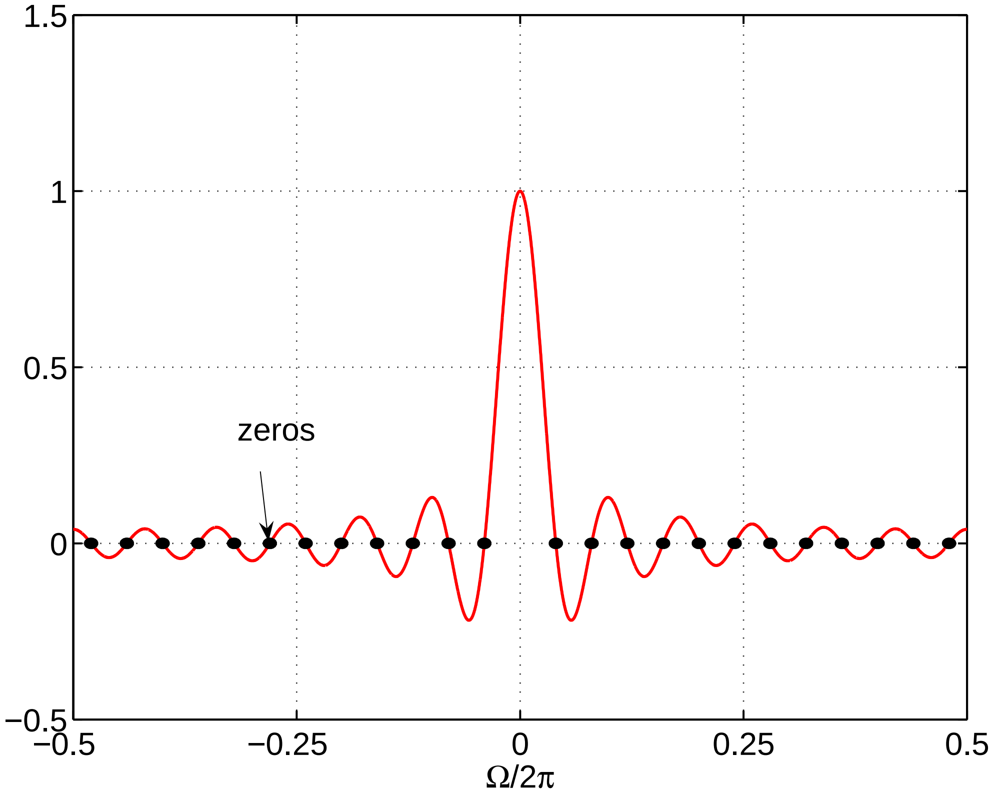

Fig. 4.1: Generating polynomial for spectrum of rectangular window

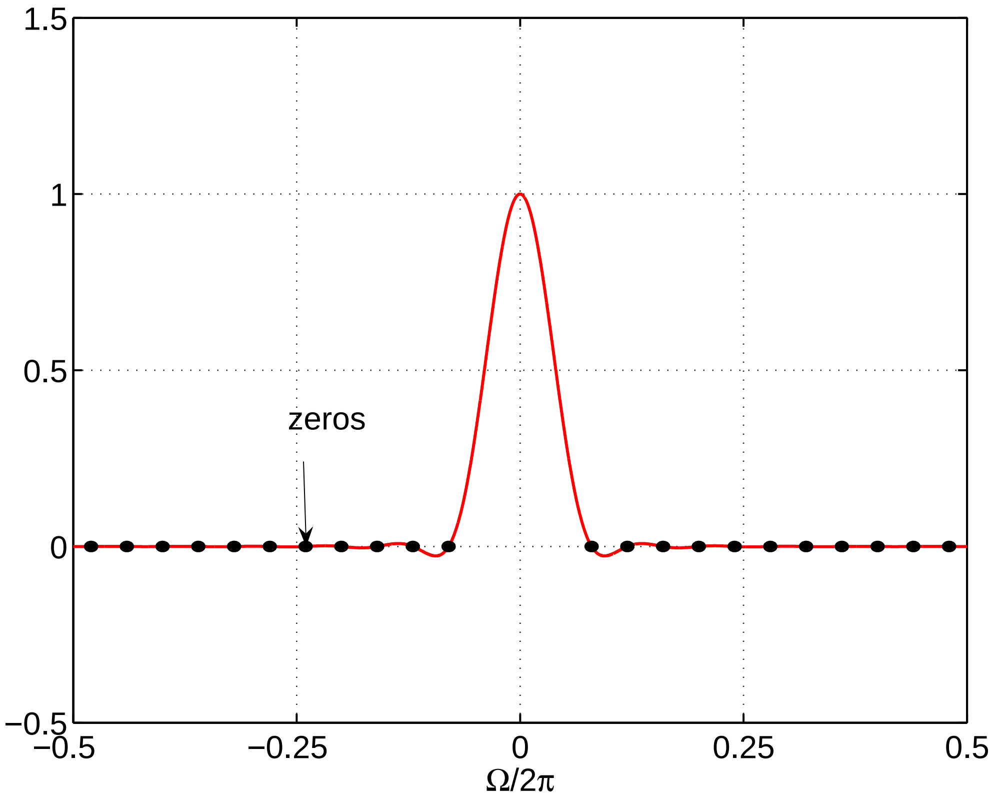

Fig. 4.2: Generating polynomial for spectrum of Hanning window

Principles

'Gap' in zeros pattern models mainlobe

Dense zeros result in high mainlobe-sidelobe-distance

Sum of single waves is represented by sum of (shifted and attenuated) generating polynomials

4.2 The 'all-poles' (AR) approach

Single pole instead of many zeros !!!

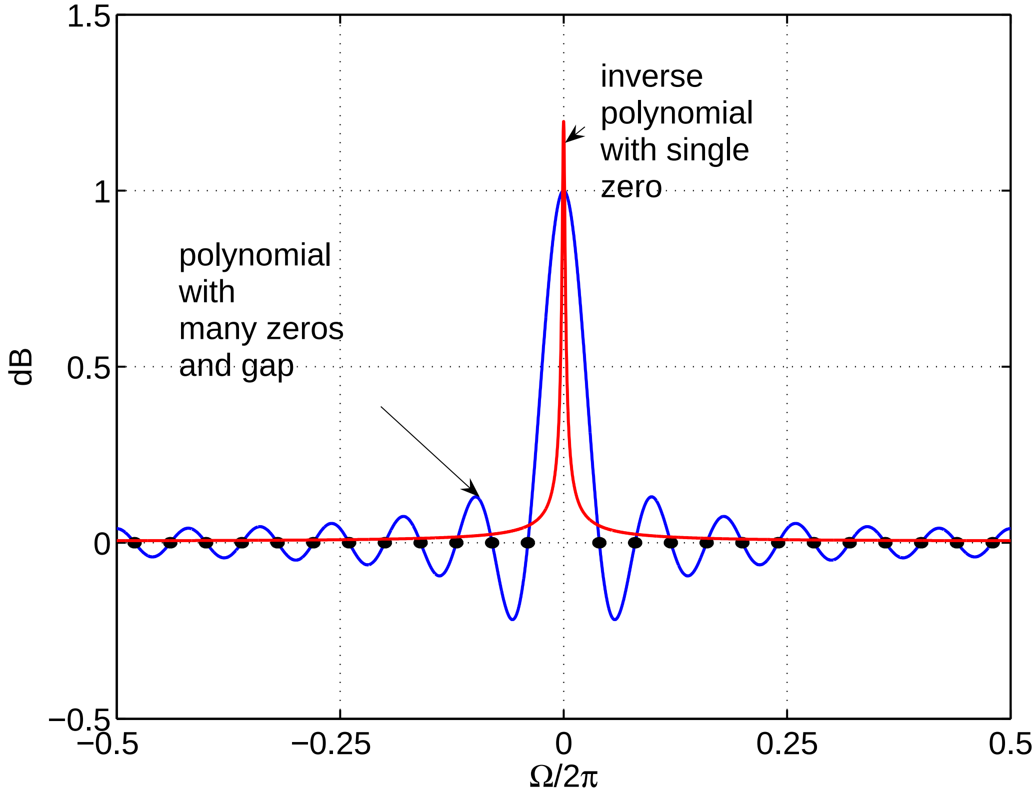

Fig. 4.3: Principle of all zeros and all poles approaches

Remarks on all-pole modeling

Pole defined by complex number

Pole-model is a nonlinear estimate for 'true' spectrum

Pole parameters computed from (estimated) autocorrelation function of spatial amplitude sequence

Decomposition (FFT) of time signal into frequencies necessary

Procedures to estimate autocorrelation function

from windowed signal

Burg procedure

forward-backward Burg procedure

and others

Experimental application of all pole modeling to setup consisting in two loudspeakers

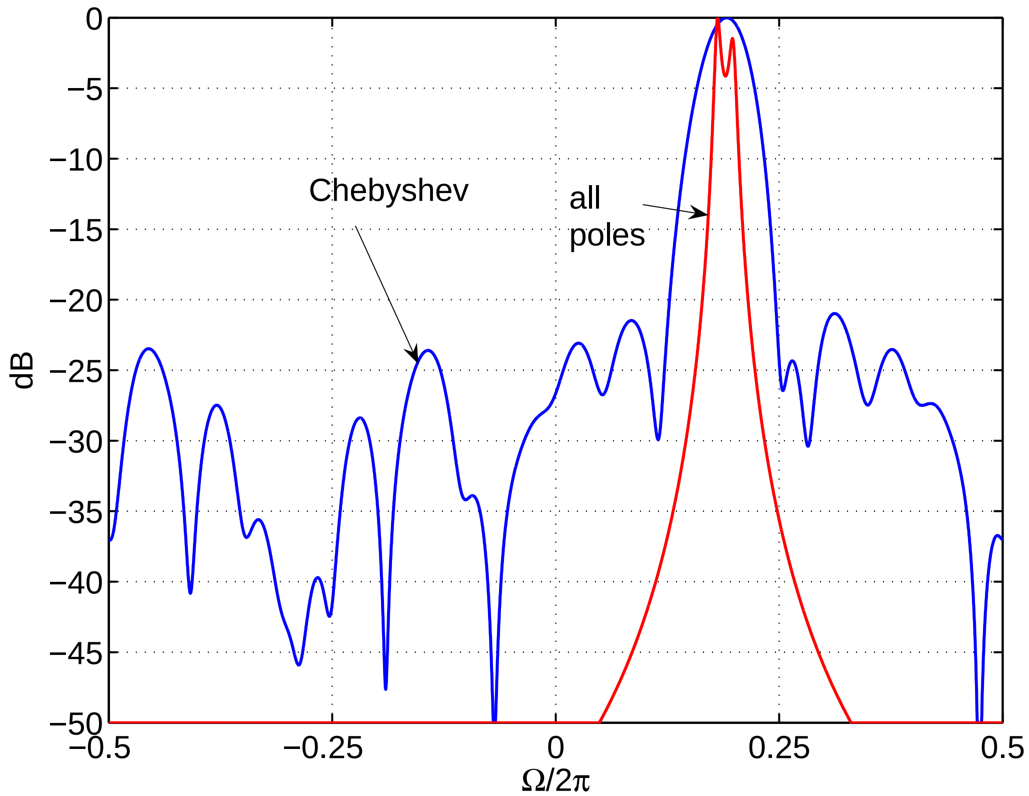

Fig. 4.4: Wavenumber spectra for Chebyshev-window (all zeros, D= 30 dB, N = 25) and all-pole-model (order=2), small source distance

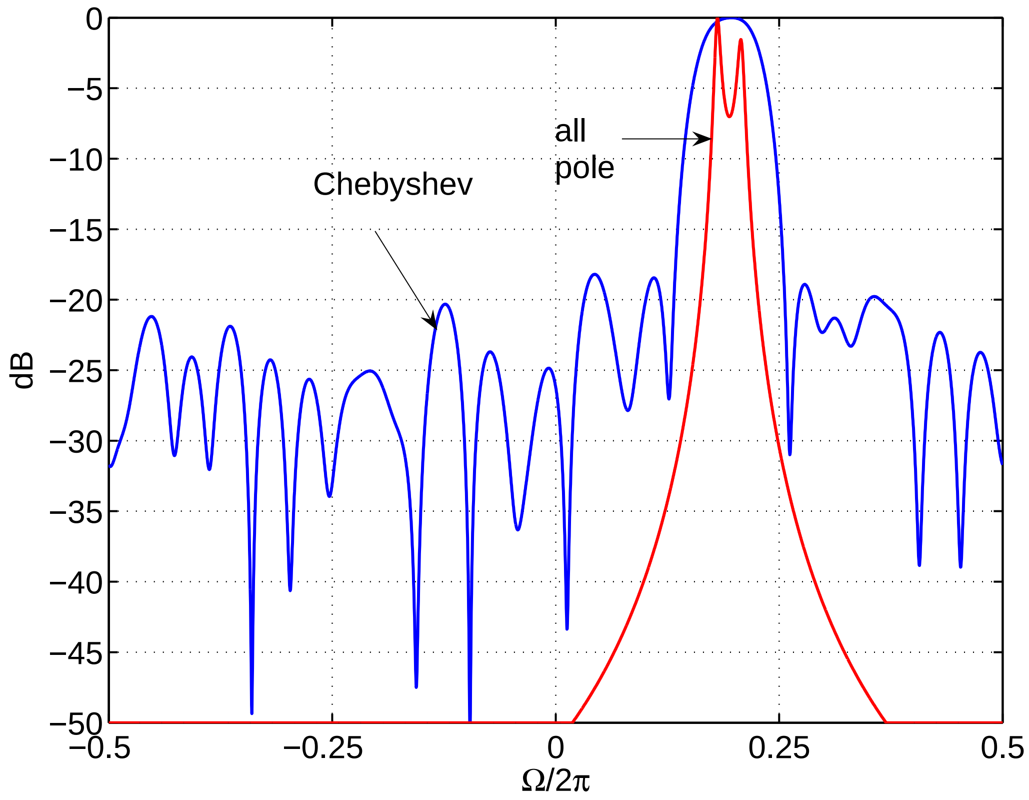

Fig. 4.5: Wavenumber spectra for Chebyshev-window (all zeros, D= 30 dB, N = 25) and all-pole-model (order=2), larger source distance

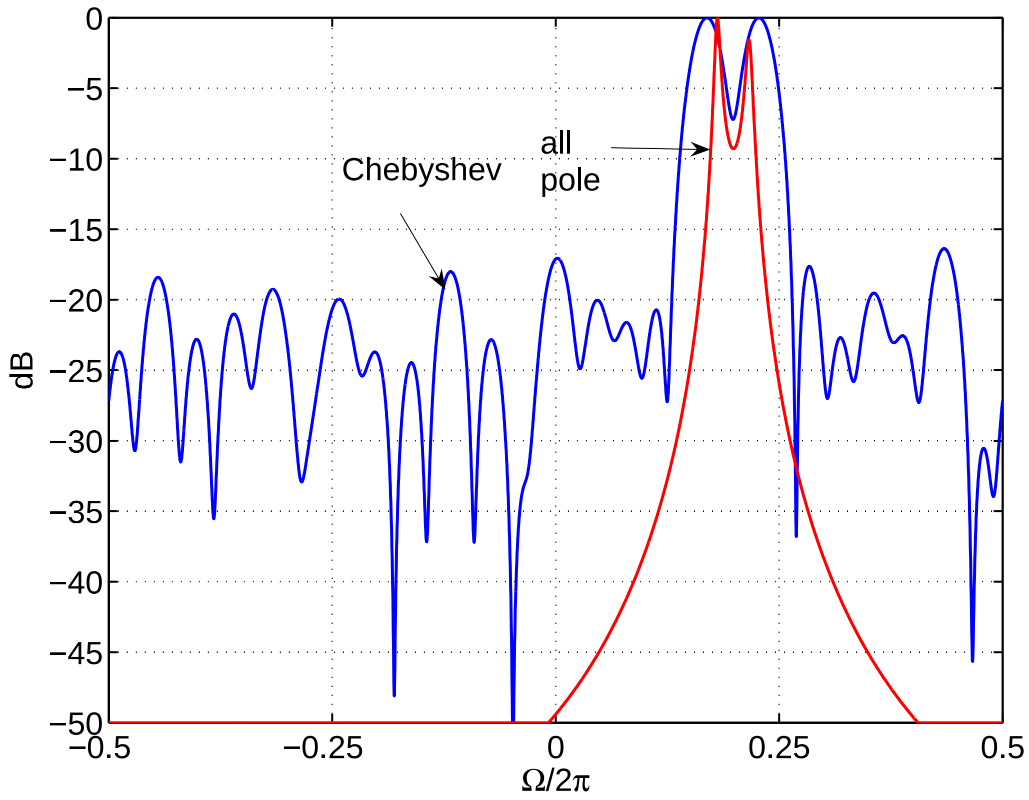

Fig. 4.6: Wavenumber spectra for Chebyshev-window (all zeros, D= 30 dB, N = 25) and all-pole-model (order=2), largest source distance used

4.3 How to estimate the amplitudes

For known wavenumbers (or frequencies): calculation of amplitudes from linear set of equations (overdetermined: minimize mean squared error)

Part 5

Summary

Phased array is a powerful tool for the detection of sources (and their distribution) and to improve signal-to-noise ratio

Conventional 'Beamforming' techniques use

- window functions and/or
- special layouts of geometrical array shape

Alternatively, nonlinear estimates for wavenumber spectra possible

Optimal solution and arrangement depending on specific application